THE SCIENTIFIC RESULTS OF THE LOW ENERGY PORTION OF A-2

Gordon Garmire
California Institute of Technology

The A-2 experiment is a collaboration between the Goddard Space Flight Center and Cal Tech with co-investigators at JPL and UCB. I would like to thank the Marshall people who have been involved these many years in the HEAO program for providing us with such a rich data base of X-ray information that we are going to be analyzing for many years. Dr. Boldt will present the extragalactic observations in the following talk and I will concentrate on some of the galactic results obtained from the experiment in this presentation. I am going to give you a little bit of the flood of data that we have already analyzed. I can assure you that there is a considerable amount of work remaining to pull out the results from all the different levels that we have within the data, so what I am giving you now is perhaps not the first look anymore, but it is sort of an intermediate stage of the analysis.

The primary goal of the A-2 experiment has been to study the diffuse background, and our particular portion of this experiment is to study the low energy diffuse background. We have collimators on our detectors which are $3° \times 3°$ and $1\ 1/2° \times 3°$, and what I would first like to show is that these detectors in fact are responding primarily to the diffuse background and not internal detector effects of different kinds which are also present. The upper squares and circles in Figure 1 are two different regions in the sky. In particular let's examine the lowest energies. At the lowest energies the sky has quite a bit of structure, and here the squares are at the polar regions (the galactic poles) and you see that at the poles, the low energy flux is considerably higher than say the flux coming from the plane of the Galaxy (circles). As you go to higher energies these two merge until up above a kilovolt, they become essentially the same. The structure that we see is predominantly in the energy range below 1 keV. This is due, we believe, to a very hot component to the interstellar medium, perhaps filling more than half the space between the stars in our Galaxy.

In Figure 2, I just want to point out a little bit of physics of this part of the spectrum because it is a bit different from what you have been hearing and will hear the rest of the day. This is the cross-section of the composite gas of the interstellar medium. Typically toward high galactic latitudes, if you invert this number, you can see out to about a kiloparsec in this spectral band. At high galactic latitudes where the disc of the Galaxy is only a hundred parsecs thick, we can actually look out of the Galaxy and see extragalactic objects. Dr. Boldt will mention a few of

those at the lower energy. At higher energies, the gas becomes completely transparent and we see everything in the Galaxy through the penetration of the X-rays.

Now our primary goal has been to map the Galaxy in different colors. Figure 3 shows the lowest energy data. This is quarter keV data and there is a tremendous amount of structure here. In fact, there is more structure than is real. That is part of the job we are currently working on, but I thought I would give you a brief progress report to show you the kind of problems we have and also a flavor of what we are seeing. The top and bottom of the map are the galactic poles which have been known for sometime, starting in 1968, I guess, with Bowyer's rocket flight which detected the bright region in the North Galactic polar area. At a longitude of about 30° toward the north is the North Polar Spur; there is a bright region in Hercules north of a longitude of 90° and there are a number of different sources. We have a 3° × 3° collimator, so these are 3° × 3° cells, which essentially do not respond very well, individually, to point sources. The cygnus Loop is at 90° longitude, the Vela diffuse region is over at 270° longitude and the Lupus region is north of the plane at 330°. The South Galactic Pole is also quite bright. There are a couple of fingers, or wisps of low energy X-ray photons coming from regions in the South in Eridanus south of 210-240° longitude and over here is the Gemini-Monoceros region north of the plane at about 200° longitude. It is quite an extended region. The stripes you see on the map are occasional electrons coming past our contamination flag, for example, that come in during solar activity. We have not eliminated those completely from this data. These data primarily summed data which have been used to search for discrete sources, so we have not taken great pains to separate out the stripes.

Now I should point out that the enhancement here in Figure 3 has been increased; the contrast has been turned up to a high level. The difference between the plane and the pole is at most about a factor of 4 in this energy band, and so these really dark regions are at most only a factor of 4 above the bulk of the region along the galactic plane. At higher energy (above 400 eV), Figure 4 shows that the sky changes completely. It is much more uniform. Again, the contrast is enhanced a bit too much. In fact I am afraid that the photographic process over-did what the computer already had done. As you can see, there is a bright region toward the galactic center. The North Polar Spur comes down near 30° again, and the rest of these dark bands are just streaks having to do with some electron effects or a little bit of bad data that came through the data filtering process. Bright objects like the Cygnus Loop and Cygnus X-2 are prominent, and just north of the plane at a longitude of 70° is a supernova remnant and some features around Cygnus X-6, as well as SS Cygni. At 275° longitude and -32° are the Large Magellanic Cloud sources, again the Vela region shows up at 265°, and the Crab is at about 185° just below the plane.

Figure 5 shows a very preliminary source map of the soft X-ray sky. The lower map is a coverage map; we had some trouble with our detector at different times and so the coverage by no means is uniform. The strongest coverage is in this very dark band corresponding to the beginning of the mission, and later on in the mission after we discovered how to play our detector without problems, we got quite a bit more coverage. Then we ran out of gas in the latter part of May 1978, so we were not able to completely fill in everything. There are still a few small gaps in our map of the sky. One thing I want to point out; at low energy the sources that we see are not at all concentrated in the plane of the Galaxy. However, you have to take out the effects of nonuniform scanning, which is a little hard to do by your eye.

If you consider the number of sources brighter than some flux level, S, then this number, S, typically follows a power law. For a disc population of sources you might find the number falls as the first power of S, and for a volume distribution the number falls as S to the 3/2 power. We find the 1/4 keV sources follow a 3/2 law pretty well down to a level of S equal to 2 HEAO-1 low energy counts. This is an energy flux of about 10^{-12} ergs/cm^2 sec for which there are about 50 sources observed. The map is still being filled in, but this is the first look at the 1/4 keV X-ray sky available from HEAO-1.

One of our first interesting surprises while we were scanning the sky was that we suddenly came upon U Geminorum when it was in outburst (Fig. 6). The optical outburst occurred actually during the upper scan in Figure 6. There was no soft X-ray flux at that time; however, the next day the soft X-ray flux became very bright and this turned out to be one of the brightest sources in the sky for us for a few days. U Geminorum is a cataclysmic variable, thought to be a white dwarf with a companion star that occasionally pours (almost periodically, in fact, on about a one hundred day period), a large amount of its outer envelope onto a white dwarf companion and thereby produces X-rays as this matter falls into the white dwarf gravitation potential. Some of the history of that object is shown in Figure 7. The optical brightening occurred at this time and here you see the soft X-rays. They became very bright and then they appeared to die away even while the optical light was still at a high level. The optical flux increased by some factor of 100 and perhaps by more than that even in soft X-rays. In the hard X-ray band it also became visible for a short time; this is in some contradistinction to other sources like EX Hydrae and SS Cygni which seem to have a hard flux during optically quiescent periods.

Another object which we saw in the very early data which I include (Fig. 8) for historical interest is the supernovae remnant MSH 14-63. At low energy we separated out a component that is centered at a slightly different celestical position. This position corresponds to the star Alpha Centauri, which is one of the closest, in fact, with Proxima Centauri, is the closest of systems of stars to us. The flux of soft X-rays we see is comparable to the that from the Sun.

Figure 10 is a light curve of Alpha Centauri and over a period of about 4 or 5 days. It was rather constant within statistics, so that we did not just observe it in a flaring state but it was something that was there rather continuously.

Figure 11 illustrates another class of object which we've detected in the low energy X-ray range. These are the RS CVn stars, named after RS Canum Venaticorum, the prototypical star in the constellation Canes Venatici. Capella, a long period member of the class, was one of the stars we saw earlier in the mission. It showed a very interesting feature in its spectrum corresponding to an iron emission of a plasma at a temperature of 10 million degrees. However, to show that these stars are not homogenous in their composition, we also have an equivalent spectrum of UX Arietus. Here we do not see any strong feature in the same part of the spectrum at all and can put a limit on the iron abundance as less than 3 percent of solar abundance at this temperature. It appears that there are quite large compositional variations in this class of object. The X-ray emitting list has grown in the class of objects as shown in Table 1. You can see that their luminosities are typically in the range of about 10^{31} ergs per second.

The neutron star systems and blackhole candidates that have been talked about by Dr. Friedman are much more luminous than the RS CVn stars, more in the range of 10^{35} -10^{37} ergs per second, so that we are talking about a class of objects here which have a much lower X-ray luminosity; however, I should point out that they are still considerably stronger than the Sun in soft X-rays, which emits typically in the neighborhood of 10^{27} ergs per second. Therefore, this is an intermediate class; these stars are rather larger in surface area than the Sun so that the surface activity is only 100 times that of the Sun rather than the 10^{4} or more that you see exhibited in their luminosity difference.

An object that we detected early in the mission was U Geminorum, a dwarf nova (Fig. 12). Later on in the mission we had a pointing at this object, and here you can see a very interesting feature; first of all the optical light curve of the object is given here in the inset, the Julian Day number is along the abscissa indicating that the outburst lasts for some 5 days. This is another tribute to the flexibility in the HEAO program which allowed us to point the spacecraft within a couple of days of the start of the outburst so that we were able to see what was happening while the outburst was in progress even though this was not in the normal pointing schedule. As you can see there is very chaotic behavior although it does appear to have a rather periodic intensity variation of around 25 sec. More about this next where we have a better example.

SS Cygni, another dwarf nova, was also observed as shown in Figure 13. This is an object which was seen in December 1977 during a quiescent period and then we had a pointing at it in June 1978 in outburst. This

pointing was done after our liquid propane gas was essentially gone. We did this pointing by using just the remaining gas phase propane in the tank. The liquid gas that we used, propane, had all vaporized and turned into gas and we were working on the residual gas left in the tank. Here you see the pulsations of the objects; this is about an 8.8 sec period and I want to emphasize that this is a new class of behavior that we've seen in the X-ray sky.

These are low energy X-rays (Fig. 14), X-rays at a quarter keV, and there are a couple of things I would like to point out. This is the pulsed fraction which goes up to about 1.0 and as you can see it goes along and it jitters a lot. That is, most of the time it is down around 0.2, but goes up to about 0.75 to 1.0. If you assume the pulses have a constant pulsation period, and then you look at the phase with respect to that period it tends to wander around and have jumps in it. Now one of the things that we discovered earlier about this source, was that in contradistinction to pulsars which have period noise, it appears from our analysis that rather these kinds of objects, which are white dwarfs, have a rather constant period but the phase jitters. You can do an analysis on the jitter by assuming a random walk behavior of the pulses with respect to time (Fig. 15). Period noise in pulsars tends to grow with an uncertainty like time to the third power. It does not get better as you add more data when you have real period noise. However, the period here does get better but what happens is that the phase changes in an unpredictable way. We have been studying this in terms on random phase analysis. We have superimposed a long stretch of data bringing each pulse successively on top of the next pulse at zero in the figure, so that each pulse is zeroed here at zero and then this oscillating curve represents some 25 oscillations of the source before and after zero. The phase noise produces an exponential decay in the amplitude of the signal as you superimpose the data at a given reference point, which is the peak of each pulse. This is because the pulses go out of phase after a characteristic number of pulses and add incoherently. One other feature of these pulses which I should emphasize, is that rather than being highly structured like neutron star pulses, these are beautiful sinusoids with less than a few percent in higher harmonics; they look very, very sinusoidal. We think what this represents is the Keplerian orbit of matter just above the surface of the white dwarf star where there is a strong interaction boundary or shock between the orbiting material and the white dwarf surface. There is a shock boundary layer that forms just above the surface and so we are seeing a period which is like the period of the inner Keplerian orbit right at the shock front. What may be happening is that the shock is being pulsed by the material coming in from the accretion disc and we see an oscillation characteristic of that time. This hypothesis plus an equation of state for the white dwarf permits us to obtain the white dwarf mass. For example, for SS cygni this gives about one solar mass, and for U Geminorum around 0.4 or 0.5 solar masses.

In Figure 16 we have analyzed four different aspects of the SS Cygni pulsations. The intensity during that observation was rather constant with a slight dropoff toward the end. The amplitude of the oscillation for SS Cygni changed quite a bit. These are individual orbits, five orbits of data plus a partial orbit. You see that the amplitude variation is rather smooth going over almost a factor of 3. The period slowly decreases during the time we are watching the source but it is not decreasing very much; it decreases something like 10^{-5} of the period per period. The strength of the phase noise changed during the interval of the observation by a factor of about 2. Figure 17 shows a similar analysis on U Geminorum. In Figure 18 the spectrum of U Geminorum is shown demonstrating how very cool the spectra of these white dwarf accreting objects are. Figure 19 is a plot of SS Cygni as a function of time just showing how the phase walks around. Here are the individual pulses; this is a superposition of about 15 pulses or so and you can see that the period just wanders around randomly. The amplitude changes and it goes through a minimum and then jumps. It could jump that way or could jump this way; I am not quite sure how it jumps, since it goes almost 180° at this point. It does that over and over again during the observations.

Figure 20 shows pulses from 4U 1626-67, a neutron star. At the higher energies, it appears that during the pulsations, which repeat every 7 sec, we see quite marked changes. Up around 19 keV you can see a strong feature which, as you go through the pulses, tends to die out and then comes back again. This is one complete cycle of pulsation for a period of 7 sec, folded over and over on itself to build up its statistics. We call this pulse phase spectroscopy. The interesting part about this source is that if you add the data from low energy all the way to high energy, it does not look pulsed. That is, the behavior of the pulsation is a very energy dependent thing. I do not have different energy bins out here to show that, but if you add all the data together the pulse seems to go away, indicating that the changes represent a scattering effect in an atmosphere of some kind where you are not losing photons but you are changing their energy distribution as the neutron star rotates around.

Figure 21 shows Hercules X-1, which is an old favorite in the X-ray business. This is a low-state spectrum when the X-ray emission is off in terms of the early analysis from Uhuru. The source is detectable in its low-state by the more sensitive HEAO-1 detectors. During the low-state, the 1.24 sec pulsations associated with the rotation of the neutron star disappear. Both the PHA and unfolded spectral fitted data show a strong iron feature at 6.4 keV. The spectrum in Figure 22 is extremely flat at the middle of the binary period but during the early part of the 1.7 day orbital period tends to steepen. There is strong iron line emission which has also been analyzed in terms of fluorescence from the atmosphere of the other star and the accretion disc. The low-state iron

line energy is 6.4 keV while during the high state it is 6.8 keV. The equivalent width changes from about 550 eV in the low-state to 300 eV in the high state, and broadens to an energy width of 1.3 keV. The narrow low-state line and shift of energy to lower X-ray energies agree with a fluorescence hypothesis.

Figure 23 shows a transient source 4U 0115+63, pulsating at a period of about 3.6 sec, which exhibits strong energy dependence during the phasing of the source as it rotates around. The two bins shown, 2 and 3, are out of ten bins for a complete rotation of the neutron star. It is clear that there is quite a bit of anisotropy in these sources as they rotate, tied in probably to a strong magnetic field. This spectrum obtained for HED III is very hard with a power law number index of 0.1.

Figure 24 shows an interesting object that has just come into prominence during the last few weeks in the press, SS433. It is an Uhuru source from sometime ago (4U 1908+05) but just began to be studied optically, and you probably have all read the press bulletins on it. In the X-ray band it shows an iron-line feature, very similar to most binary X-ray sources, so it does not seem to reveal anything special in the X-ray band.

In conclusion, I've shown a number of the interesting galactic phenomena at high energy which have been studied using the HEAO-1 detectors. I've omitted a discussion of supernova remnants for a lack of time, but I should just mention that we have discovered about nine or ten new remnants, almost doubling the pre-HEAO-1 number. Dr. Boldt will now continue with a presentation of the extragalactic results.

BIBLIOGRAPHY

Cash, W., Bowyer, S., Charles, P., Lampton, M., Garmire, G., and Riegler, G.: Astrophys. J. Lett., 223, L21, 1978.

Cordova, F.: Ph.D. thesis, California Institute of Technology, 1979.

Cordova, F. A., Chester, T. J., Tuohy, I. R., and Garmire, G. P.: to be published in Astrophys J., 1979.

Cruddace, R., Paresce, F., Bowyer, C. S., and Lampton, M.: Astrophys. J., 187, 497, 1974.

Hall, D. S.: In Multiple Periodic Variable Stars, ed. W. S. Fitch (Reidel: Dordrecht), 1976.

Marshall, F. E., Swank, J. H., Boldt, E. A., Holt, S. S., and Serlemitsos, P. J.: Astrophys. J. Lett., 230, L145, 1979.

Mason, K. O., Cordova, F. A., and Swank, J. R.: Proc. of the COSPAR Symp., Insbruck, Austria, June 1978.

Nugent, J., and Garmire, G.: Astrophys. J. Lett., 226, L83, 1978.

Pravdo, S. H., Boldt, E. A., Holt, S. S., Rothschild, R. E., and Serlemitsos, P. J.: Astrophys. J. Lett., 225, L53, 1978.

Pravdo, S. H., White, N. E., Boldt, E. A., Hold, S. S., Serlemitsos, P. J., Swank, J. H., Szymkowiak, A. E., Tuohy, I. R., and Garmire, G.: submitted to Astrophys. J., 1979.

Rose, L. A., Pravdo, S. H., Kaluzienski, L. J., Marshall, F. E., Holt, S. S., Boldt, E. A., Rothschild, R. E., and Serlemitsos, P. J.: Astrophys. J., 231, 919, 1979.

Rothschild, R., Boldt, E., Holt, S., Serlemitsos, P., Garmire, G., Agrawal, P., Riegler, G., Bowyer, S., and Lampton, M.: Space Sci. Instr., 4, 279, 1979.

Walter, F., Charles, P., and Bowyer, C. S.: Astrophys. J. Lett., 225, L119, 1978.

Walter, F., Charles, F., and Bowyer, C. S.: Astron. J., 83, 1539, 1978.

TABLE I

Name	Date (UT)	L_x (erg s^{-1}) (.2-2.8 keV)	$D^{(1)}$ (pc)
UX Ari	1977 17-22 August	$2.1 \pm .04 \times 10^{31}$	50
HR 1099	1977 17 August 1978 9-10 February	$1.1 \pm .1 \times 10^{31}$	33
RS CVn	1977 20 December	$1.1 \pm 2 \times 10^{32}$	145
RS CVn	1977 19,21 December	$< 4.4 \times 10^{32}$ (3σ)	145
AR Lac	1977 19-22 December	$1.5 \pm 1 \times 10^{31}$	50
LX Per	1977 21-23 August	$2.2 \pm .2 \times 10^{31}$	145
RW UMa	1977 24 November	$9.6 \pm .7 \times 10^{32}$	150
RW UMa	1977 22,23 November	$< 5.7 \times 10^{32}$ (3σ)	150
α Aur[2]	1977 14-16 August	4×10^{30}	14
HK Lac	1977 19-22 December	$1.3 \pm 1 \times 10^{32}$	150
σ Gem	1977 14-16 October	$1.3 \pm .1 \times 10^{32}$	150
Z Her	1977 21-23 September 1978 19-20 March	$< 9.8 \times 10^{30}$ (3σ)	85
SZ Psc	1977 11-12 December	$< 1.4 \times 10^{32}$ (3σ)	100
TY Pyx	1977 22-23 November	$< 8.8 \times 10^{30}$ (3σ)	85
HR 5110	1977 24-26 December	$< 4.4 \times 10^{30}$ (3σ)	50

(1) Hall (1976)

(2) Cash et al. (1978)

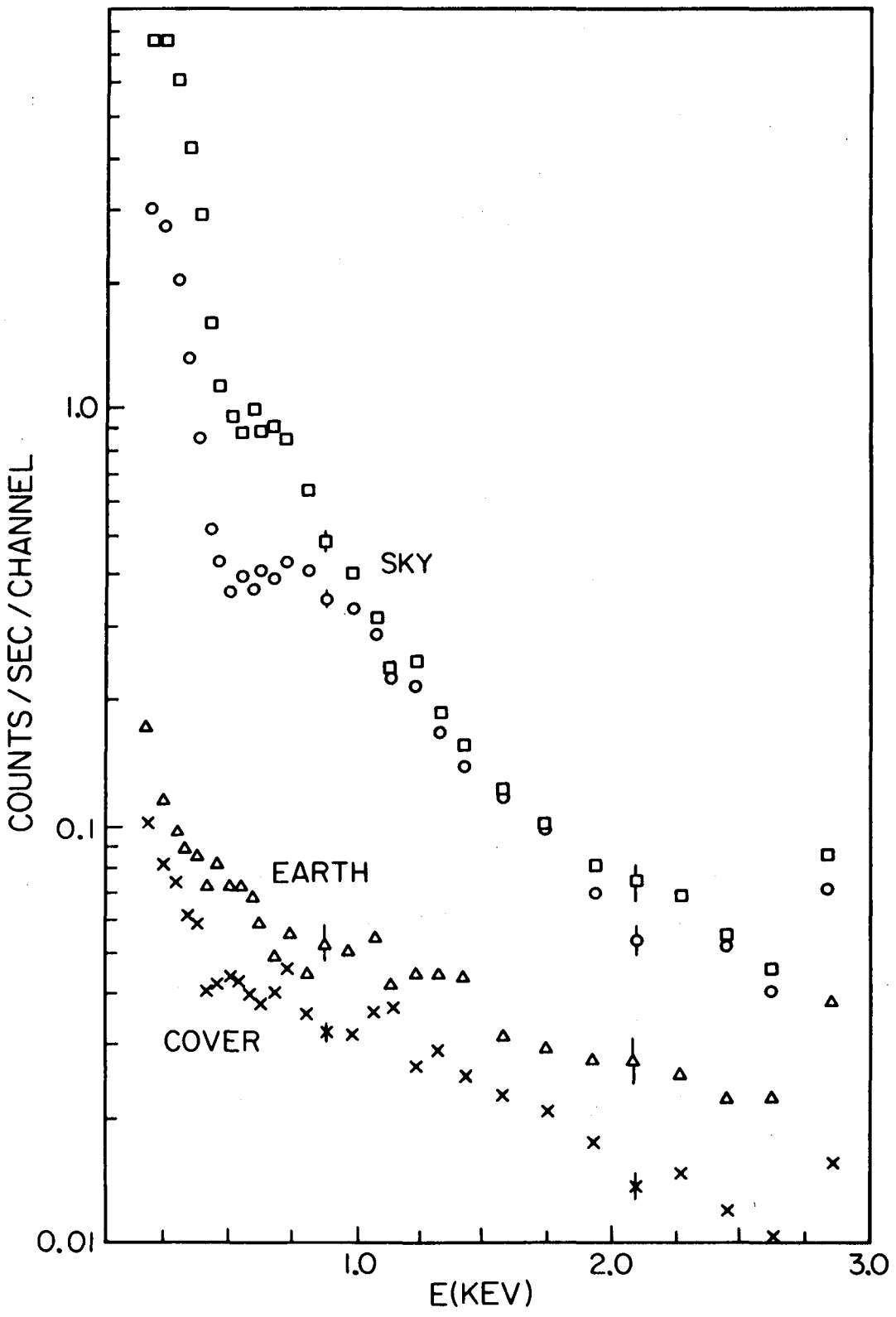

Figure 1. The pulse height spectrum of events recorded from the galactic pole (□), the galactic plane (o), the Earth and the detector with the acoustic door closed. The excess Earth events over the cover-closed events are probably electron background.

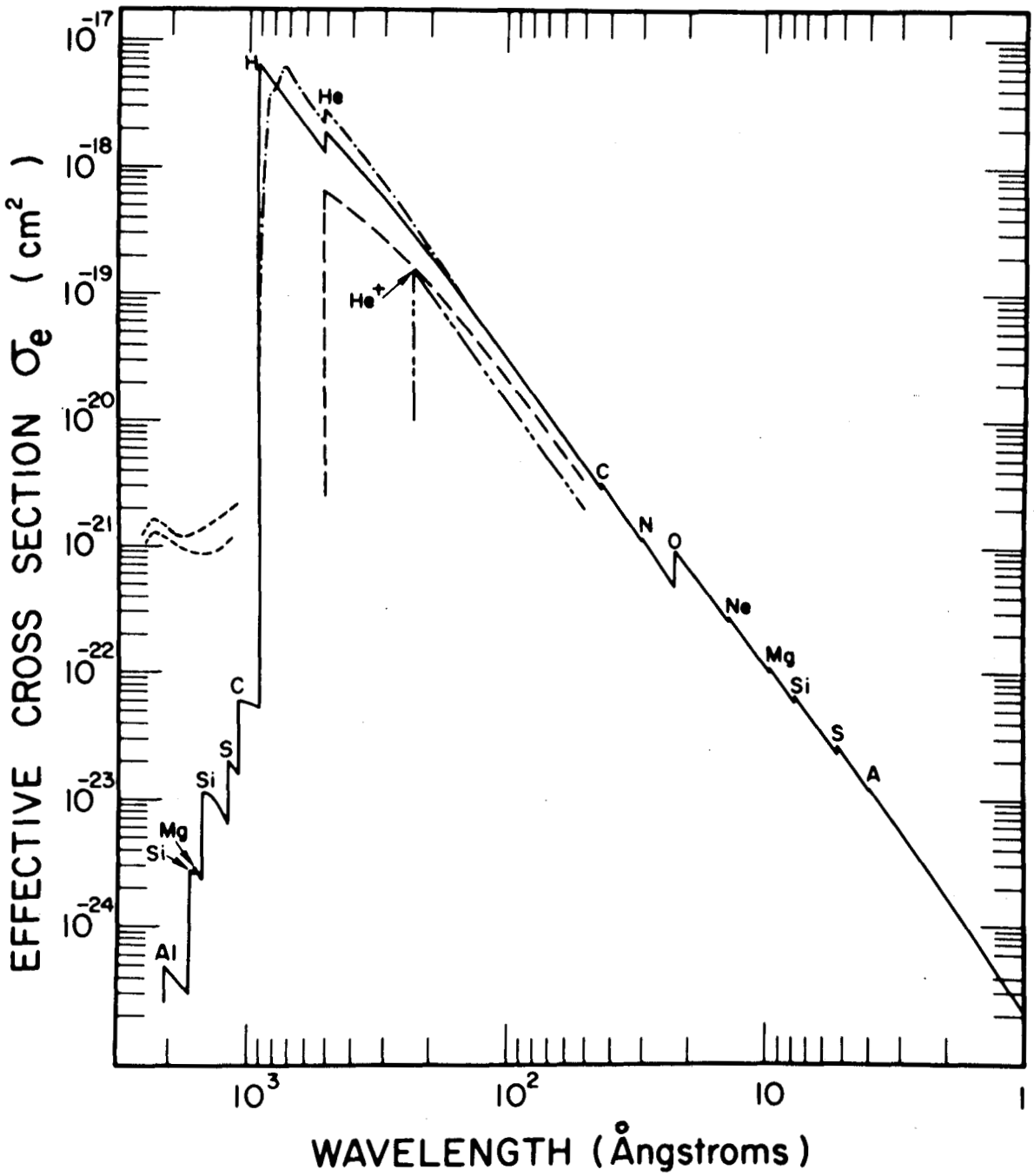

Figure 2. This is a figure from Cruddace et al. (1975), which shows the absorption properties of the interstellar medium. The density of gas in the galaxy is about 0.5 atoms/cm^3, so at 10 Å we can "see" out to a distance of about 7 kps, and at 50 Å out to a distance of about 80 pc.

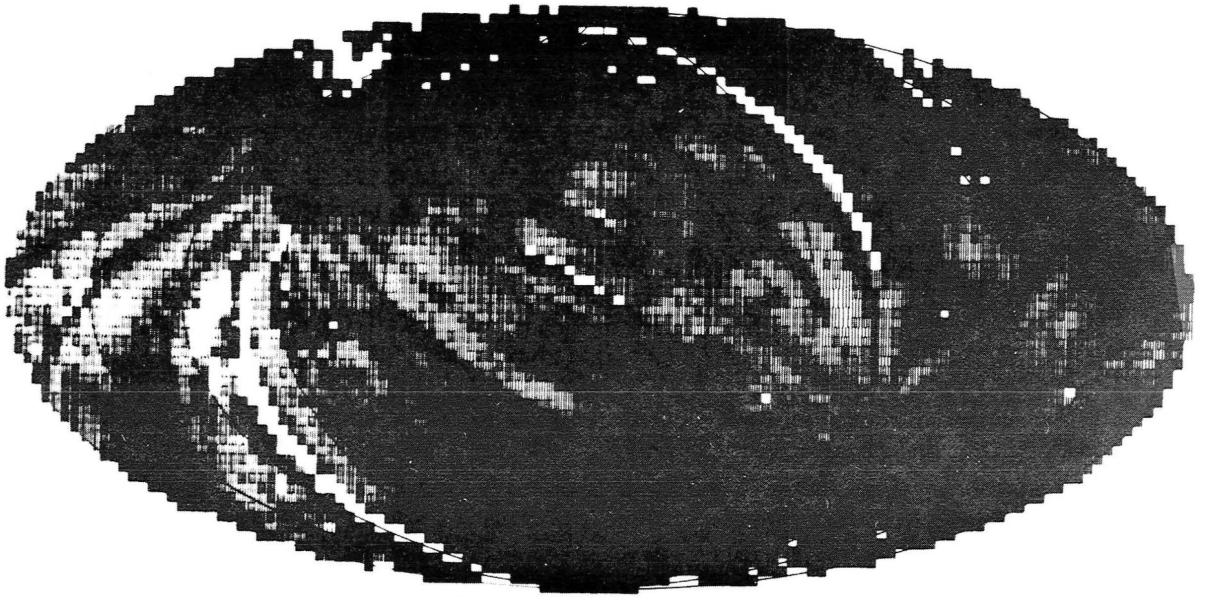

Figure 3. The 1/4 keV sky. Dark areas are brighter. The North Galactic Pole is at the top and 0°, the Galactic Center, is at the center. Light streaks are missing data. Dark streaks are electron contamination.

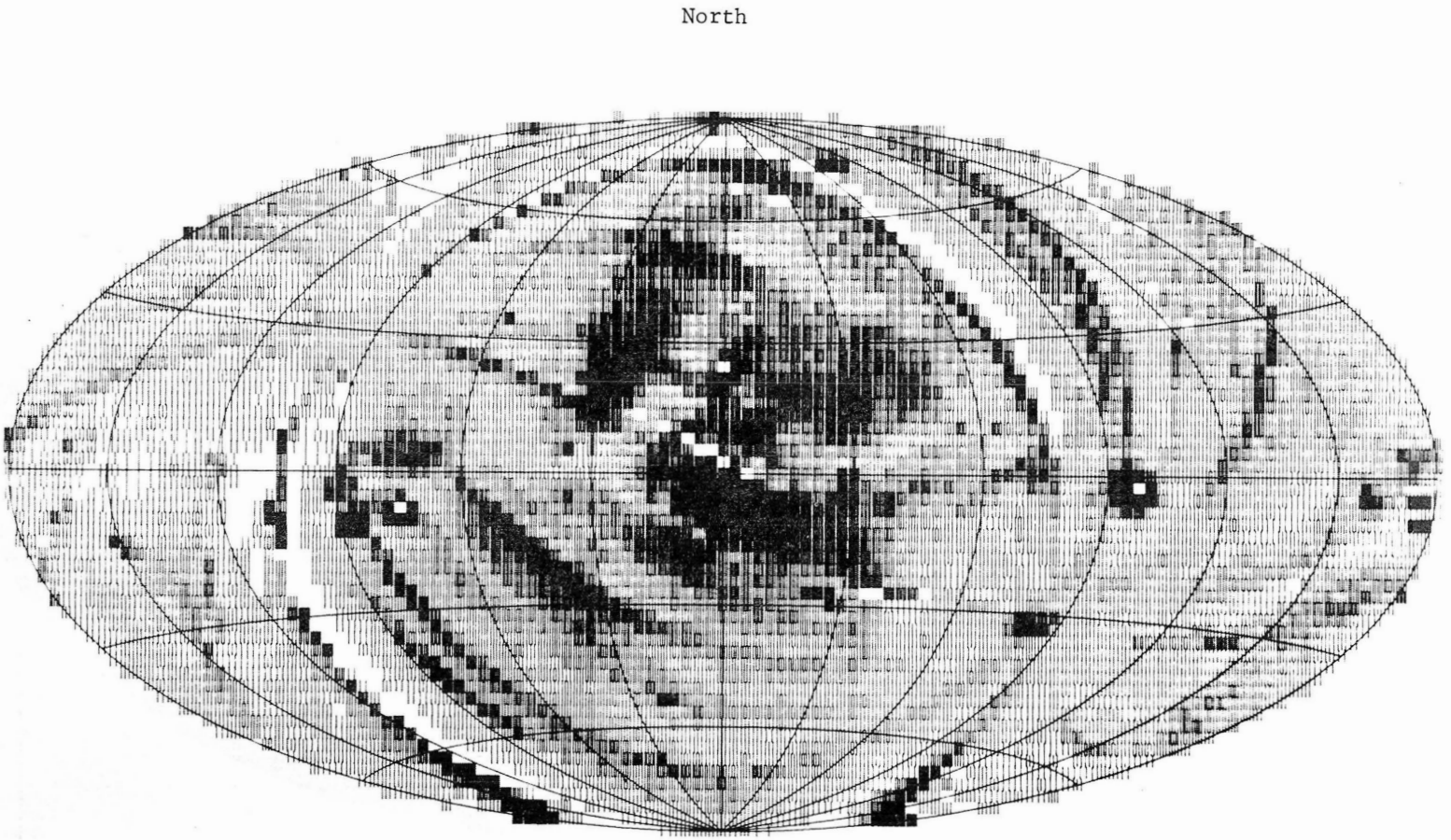

Figure 4. The > 0.4 keV sky. The same description as for Figure 3.

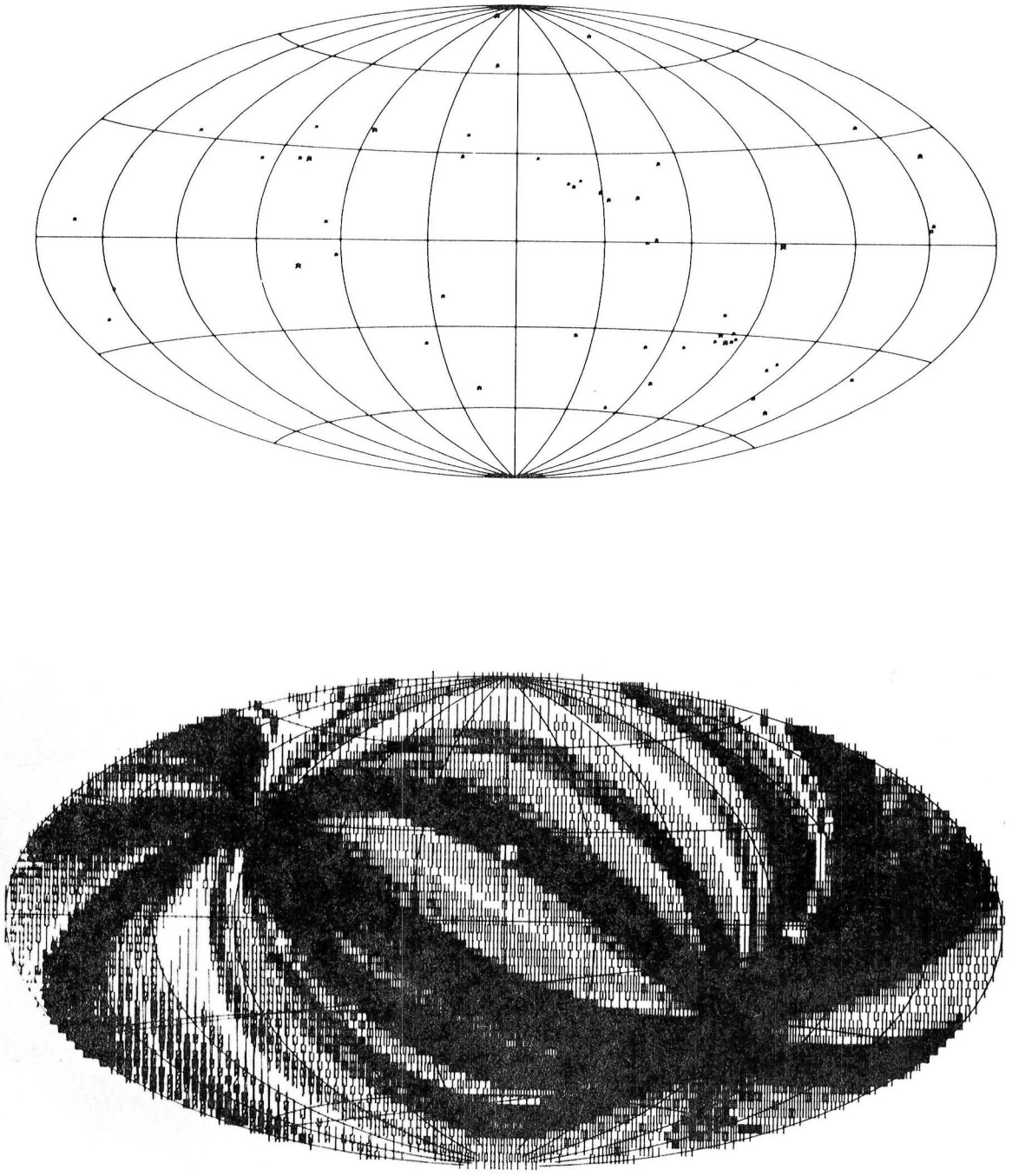

Figure 5. The upper figure is the distribution of 1/4 keV sources observed from HEAO-1. The lower curve is the exposure map, darker being more exposure. The square hole at 0° longitude and +20° latitude is Sco X-1 and is an artifact of the way the exposure map was created.

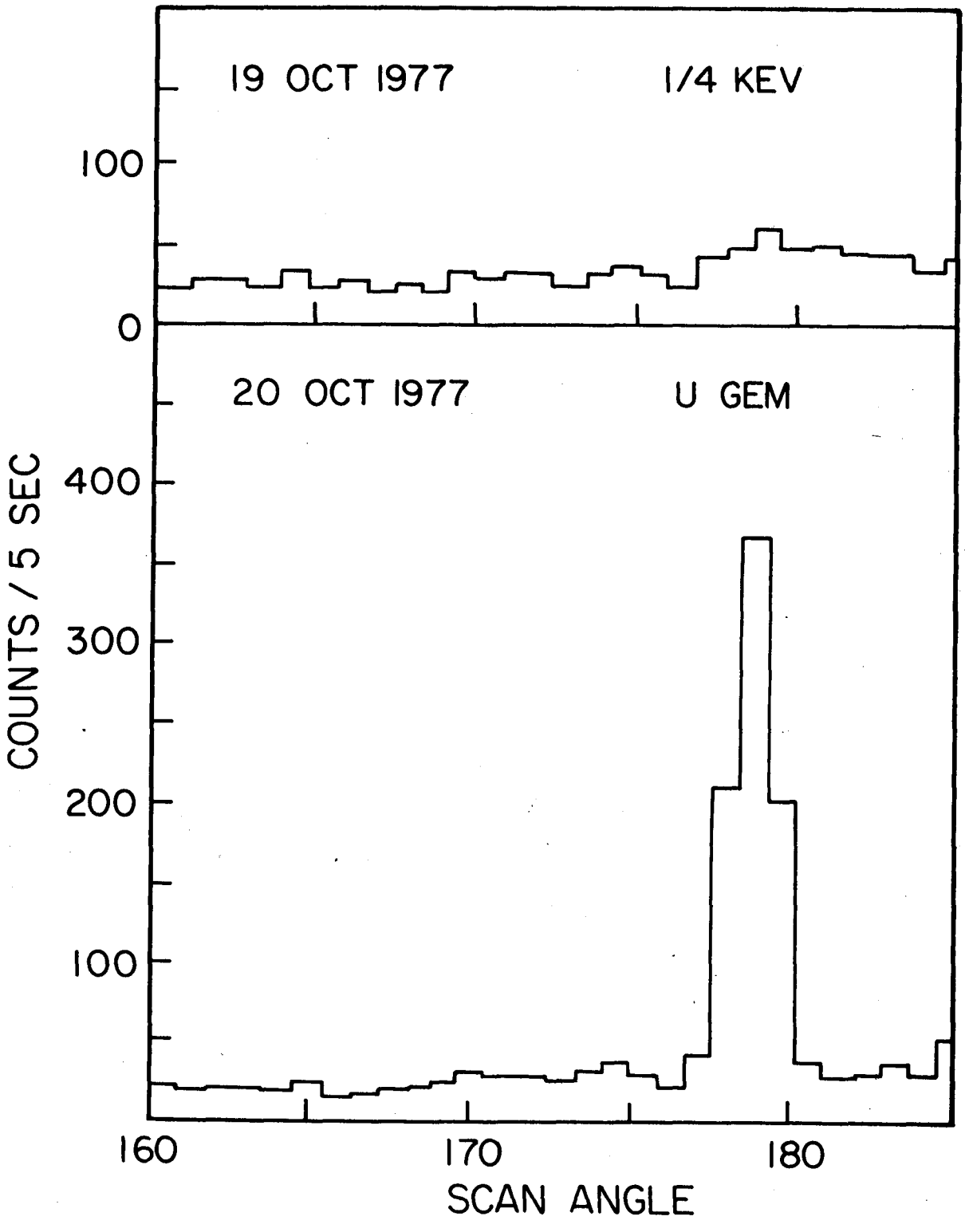

Figure 6. The upper curve is the 1/4 keV counts versus scan angle. The lower curve is the same one day later showing the tremendous increase in U Gem.

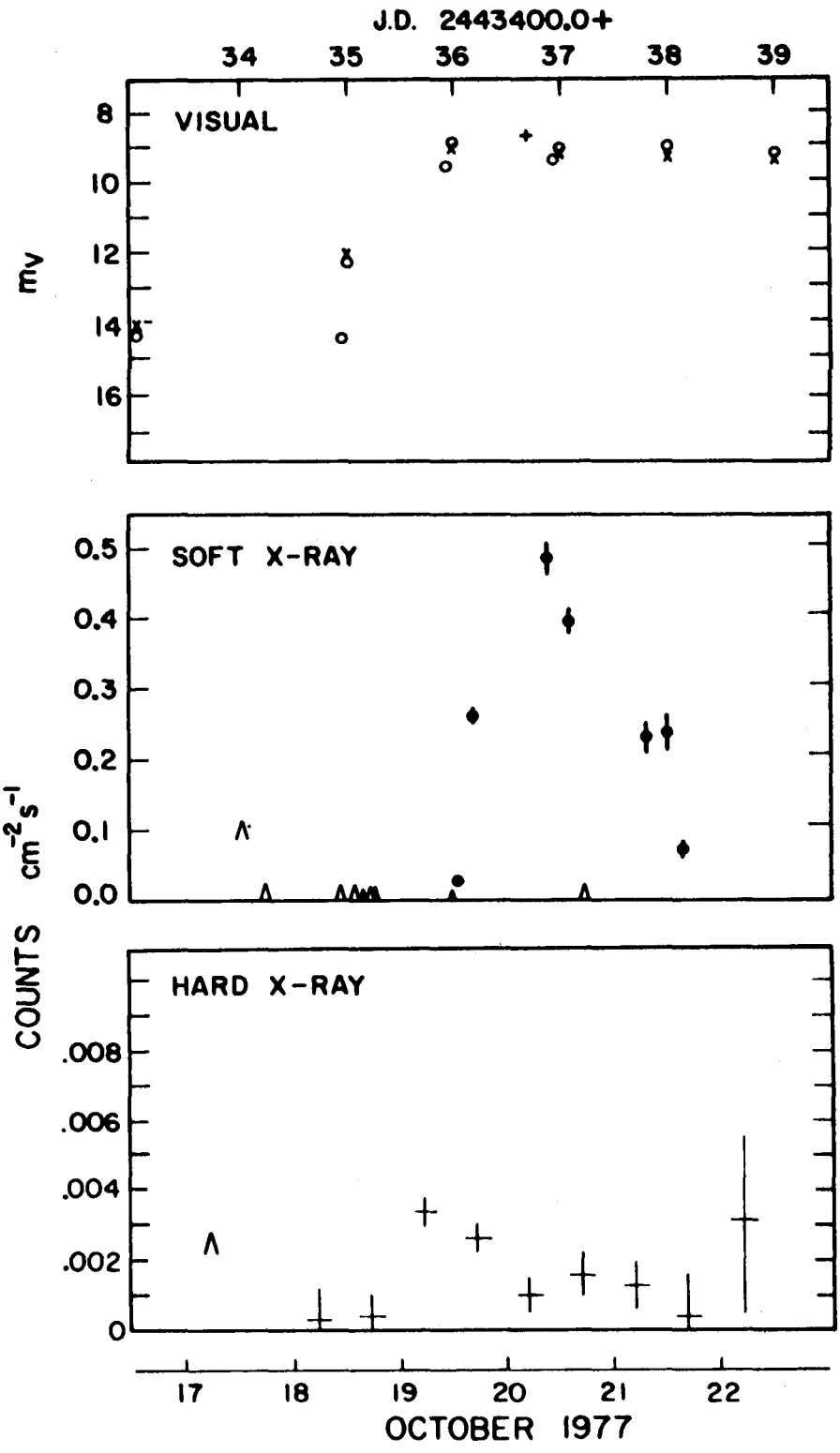

Figure 7. The visual intensity (upper), soft X-ray intensity and hard X-ray intensity of U Gem as function of time from Mason et al. (1979).

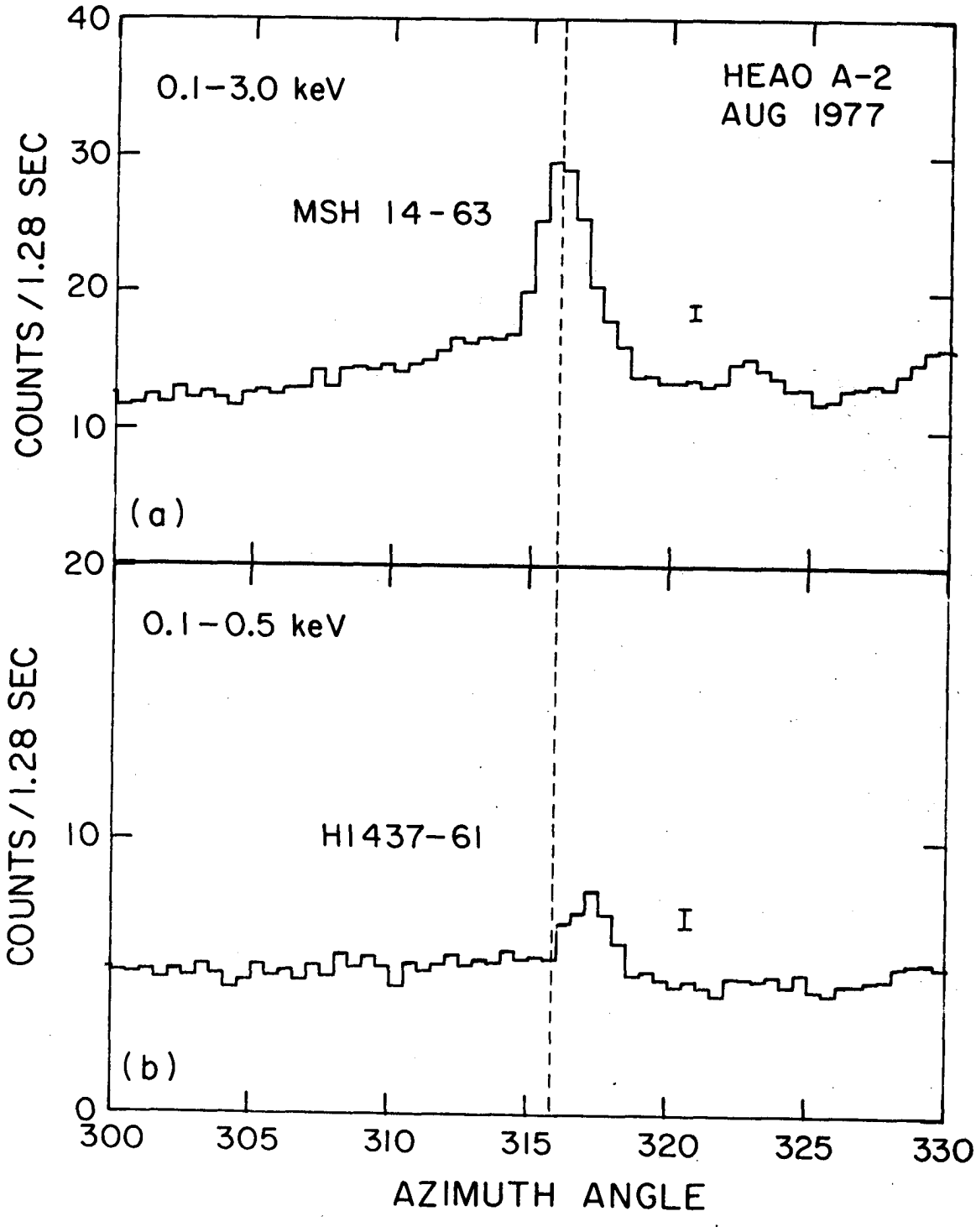

Figure 8. The scan over the region of MSH 14-63 (upper) and the displacement of the counts at low energy due to presence of a separate soft X-ray source.

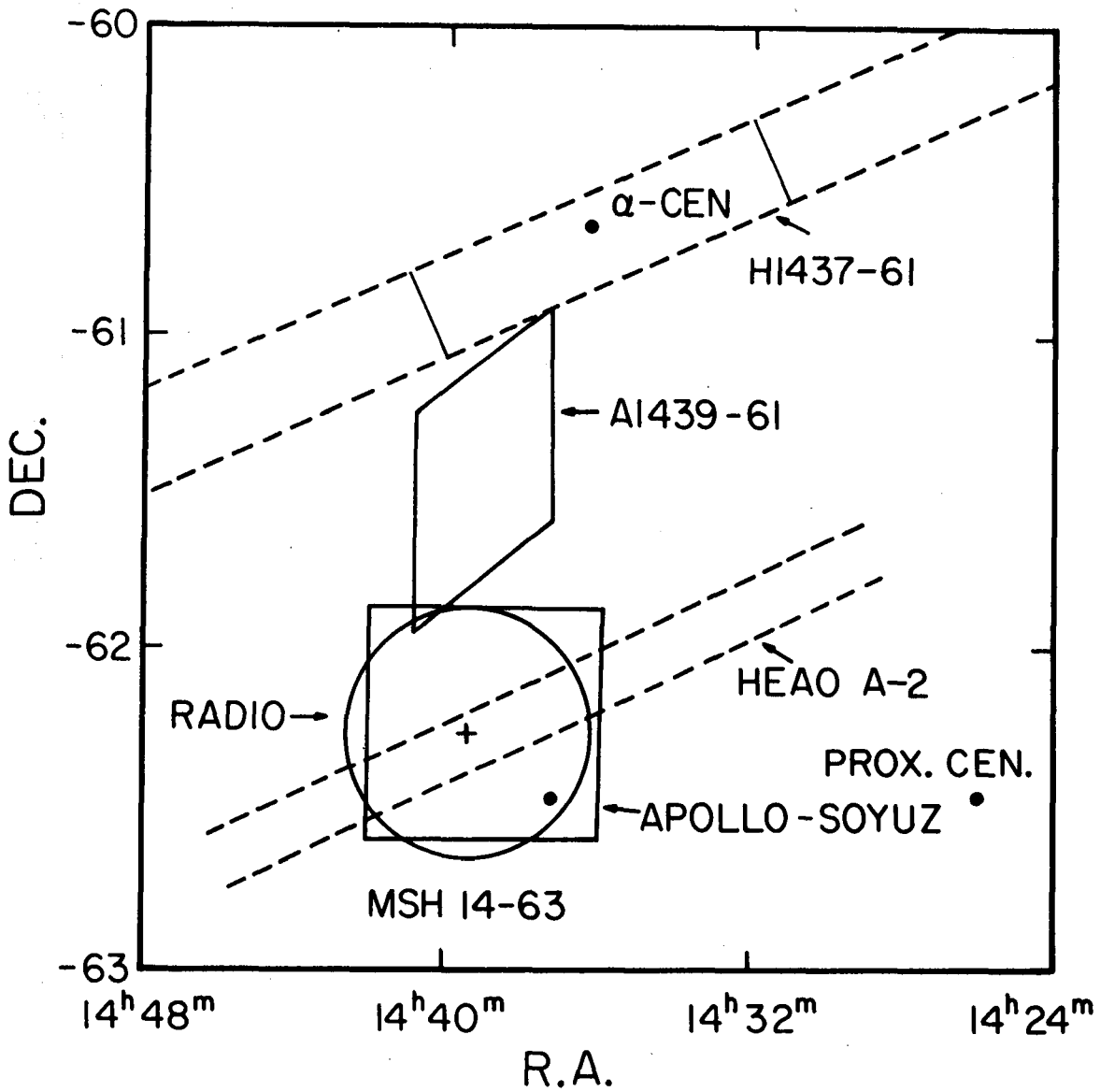

Figure 9. The position of the new soft source relative to some other sources.

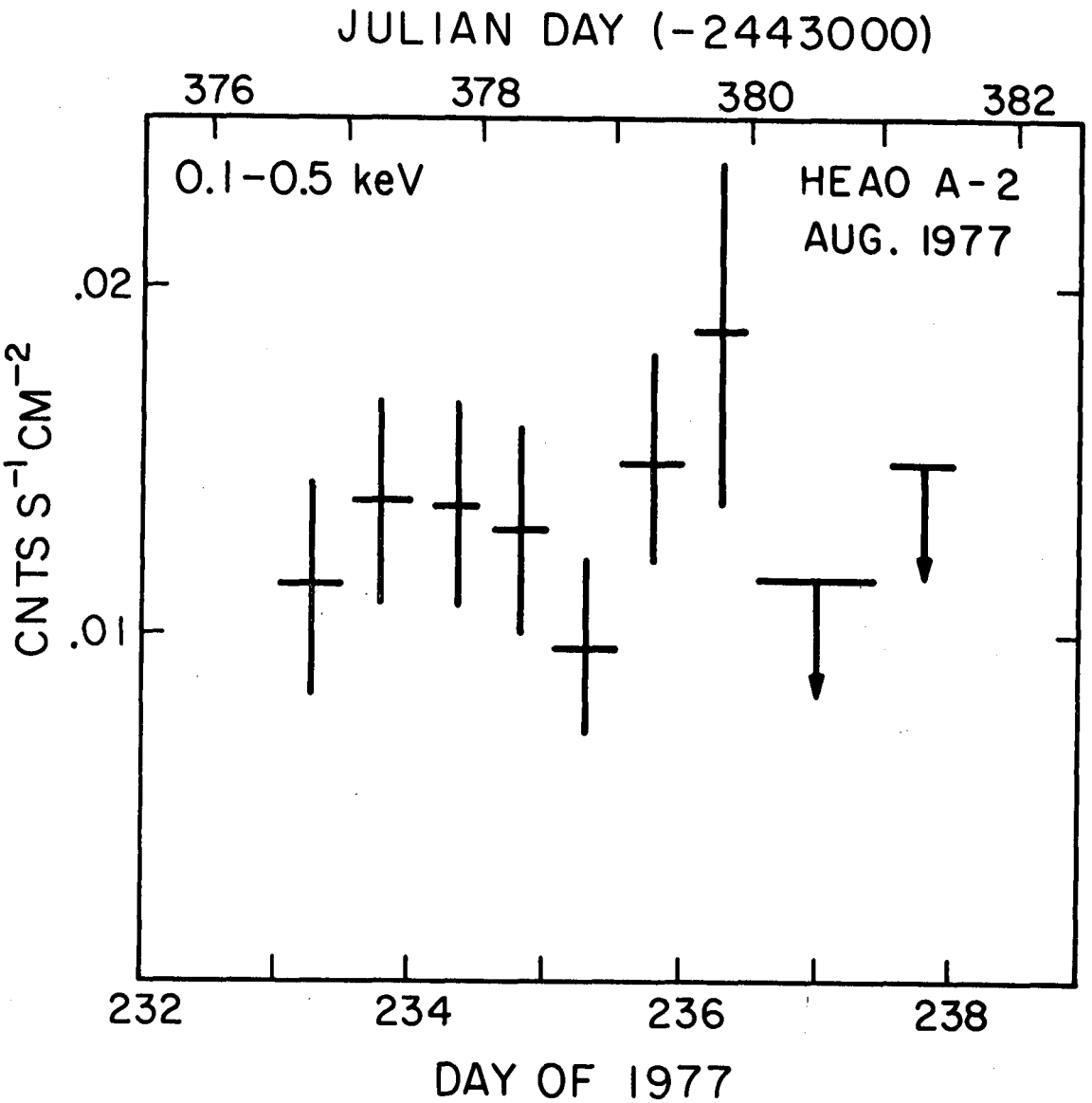

Figure 10. The intensity of α-Cen as a function of time in 1977 while it was scanned.

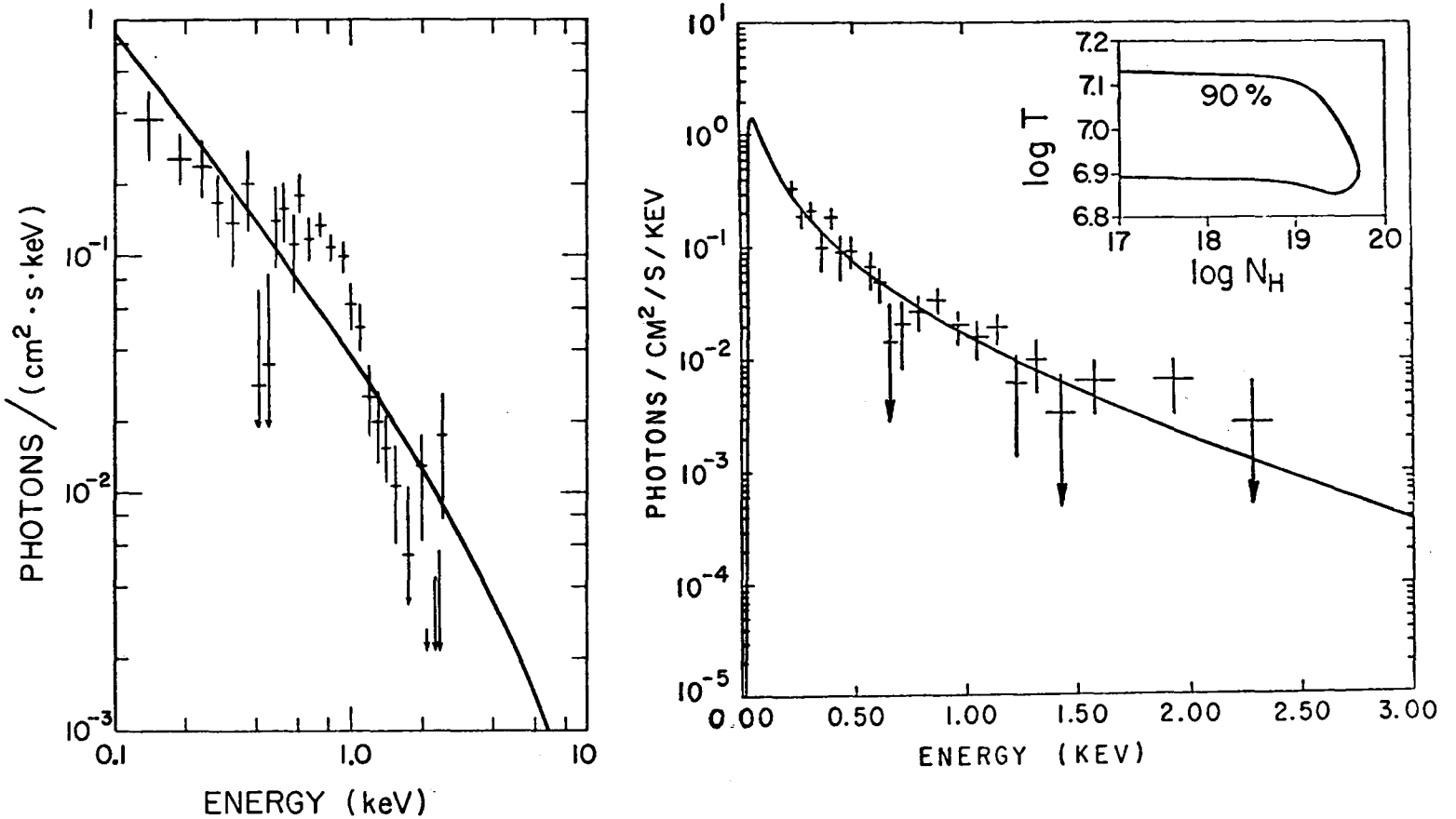

Figure 11. The Capella spectrum on the left showing the enhancement of about 800 eV due to ionized iron emission at a temperature of about 10^7 K from Cash et al. (1978). The right hand figure is UX Arietus showing no iron emission even though the temperature is ~ 107 K also implying a decreased iron abundance, (from Walter et al. 1978b, Table I).

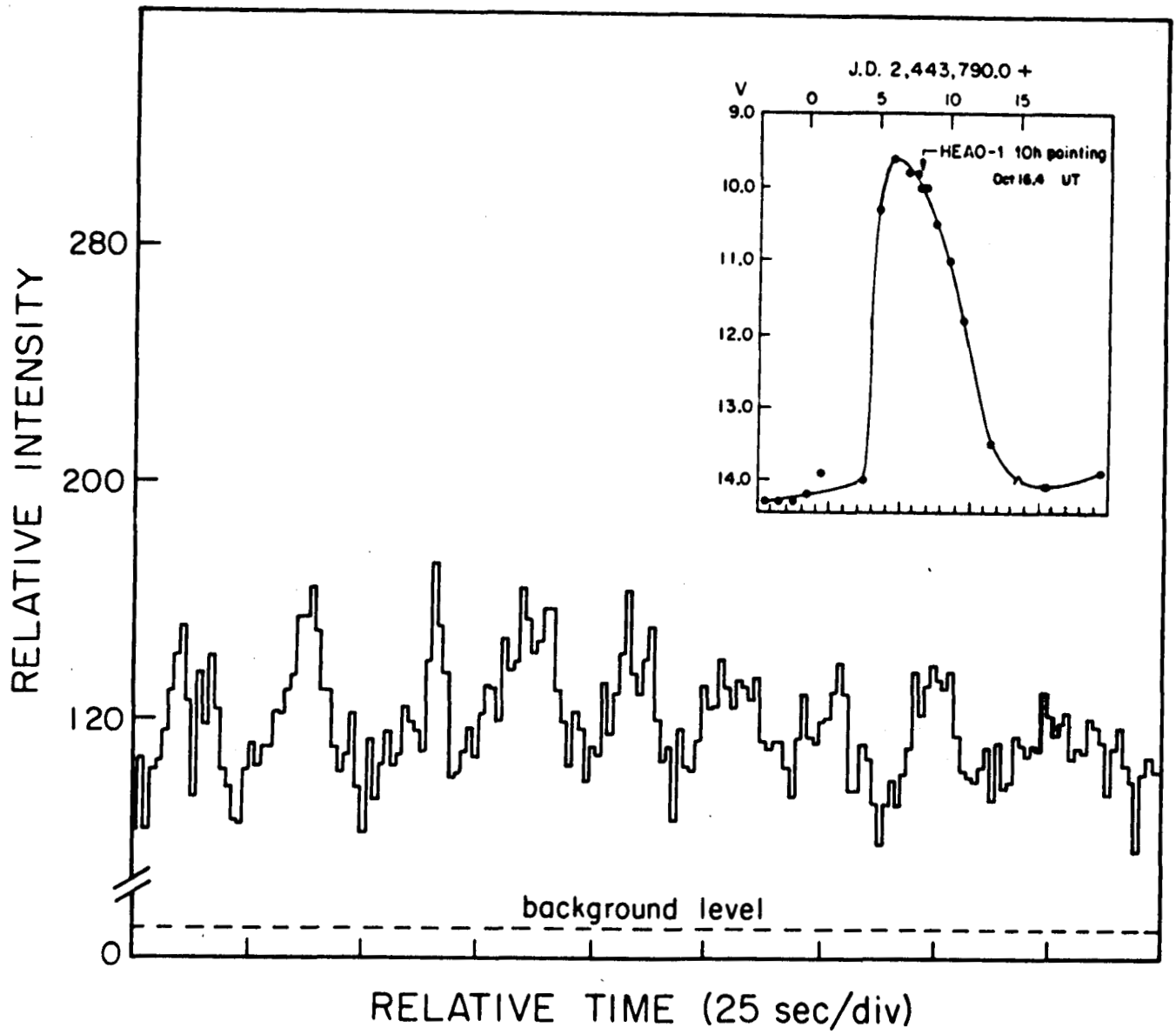

Figure 12. The pointed observation of U Gem in 1978. The inset is the optical light curve and the lower curve is a portion of the X-ray data.

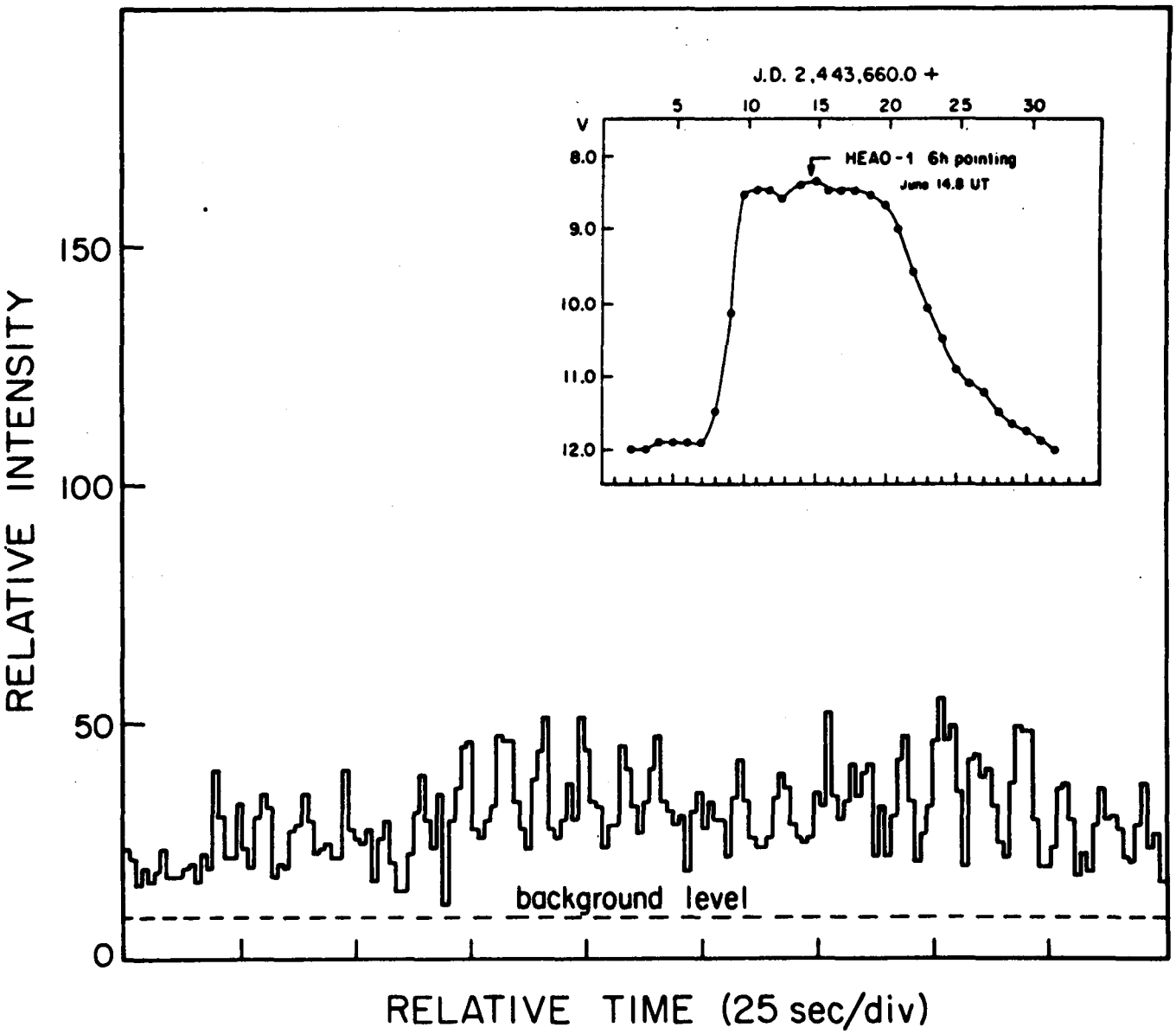

Figure 13. The pointed observation of SS Cygni in 1978. The inset is the optical light curve and the lower curve is a portion of the X-ray data.

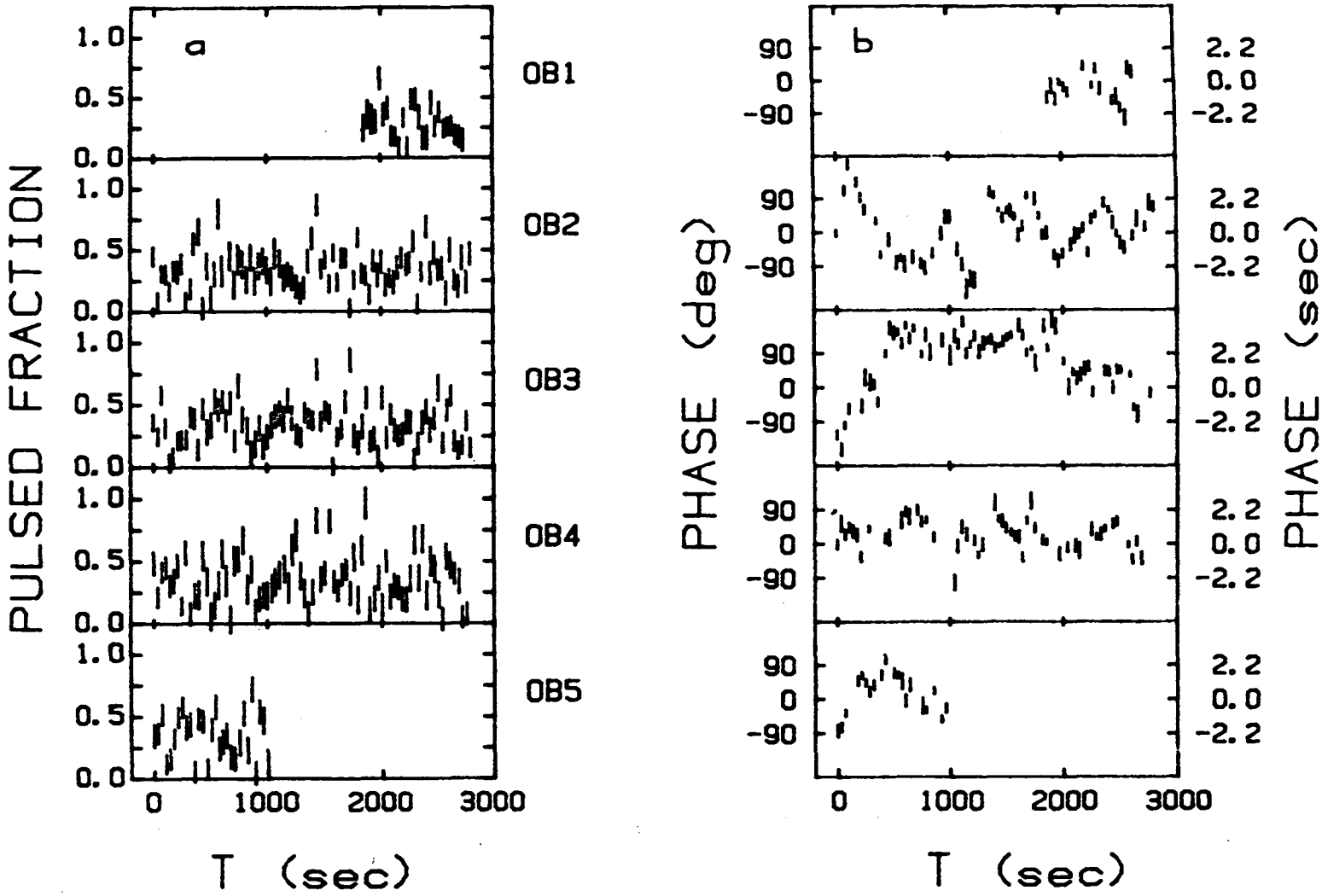

Figure 14. The pulsed fraction observed in SS Cygni (left) for each orbit binned every 41 seconds for each orbit, and the phase relative to a constant period for each orbit (right) from Cordova (1979).

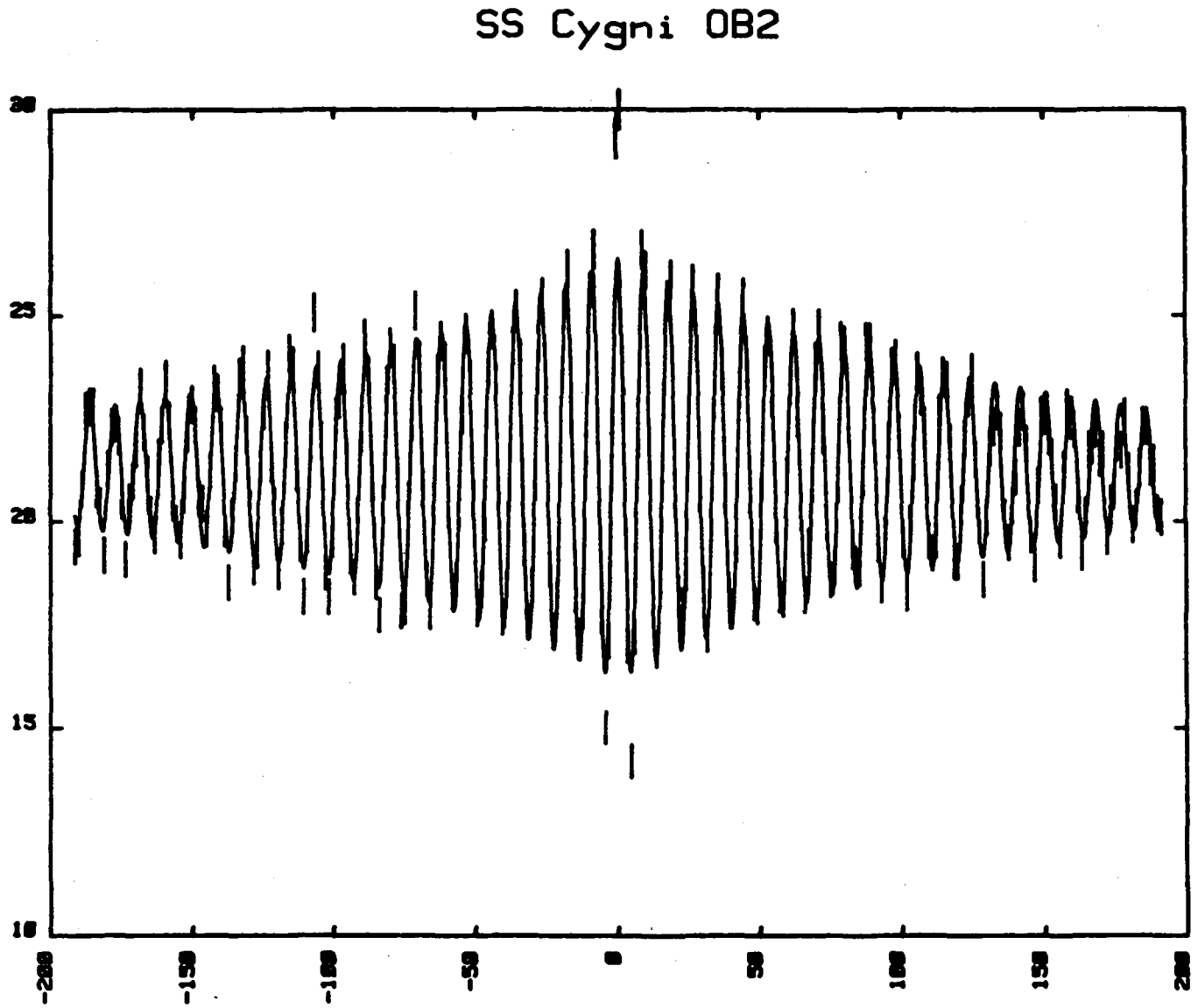

Figure 15. The superposition of pulse trains from SS Cygni. A pulse is centered with peak intensity at zero and all pulses on either side are recorded. Then the train is moved one pulse later and again all the pulses are added. A sine curve with exponentially decreasing amplitude with time is fitted to the data points.

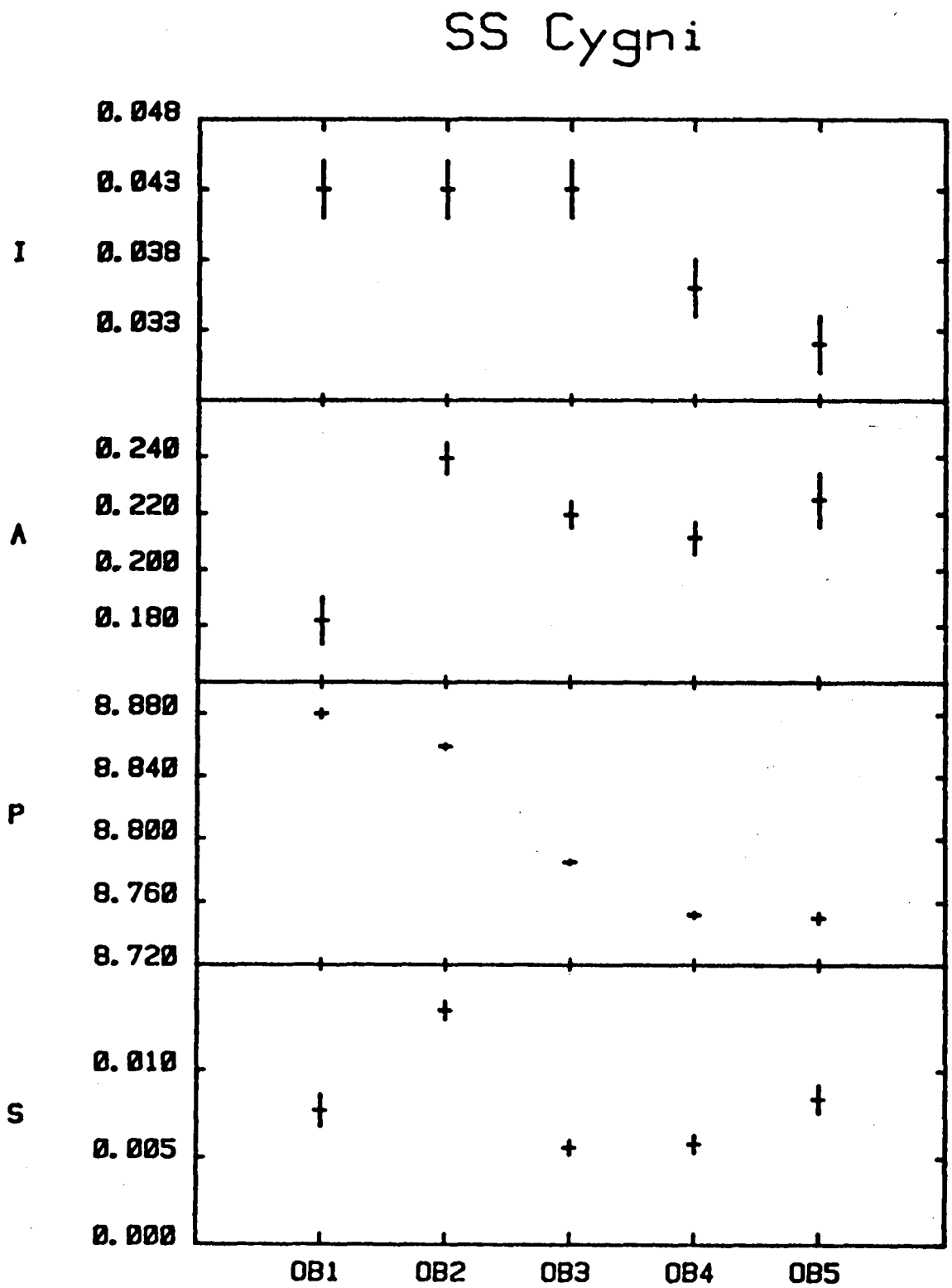

Figure 16. The intensity versus orbit number of SS Cyg (upper), amplitude of pulsations, A, period, P, and random walk strength, S.

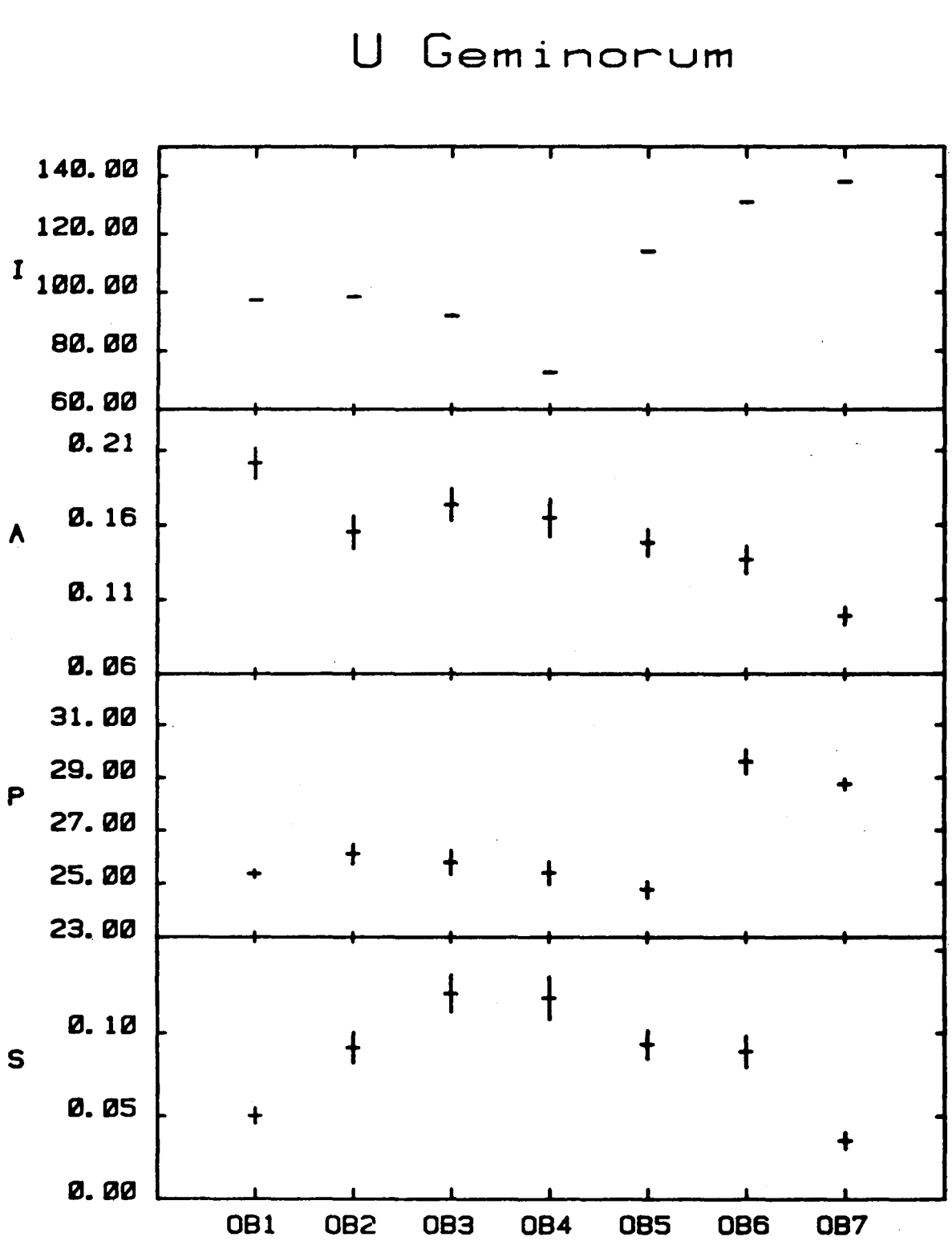

Figure 17. The intensity versus orbit number of U Gem (upper), amplitude of pulsations, A, period, P, and random walk strength, S.

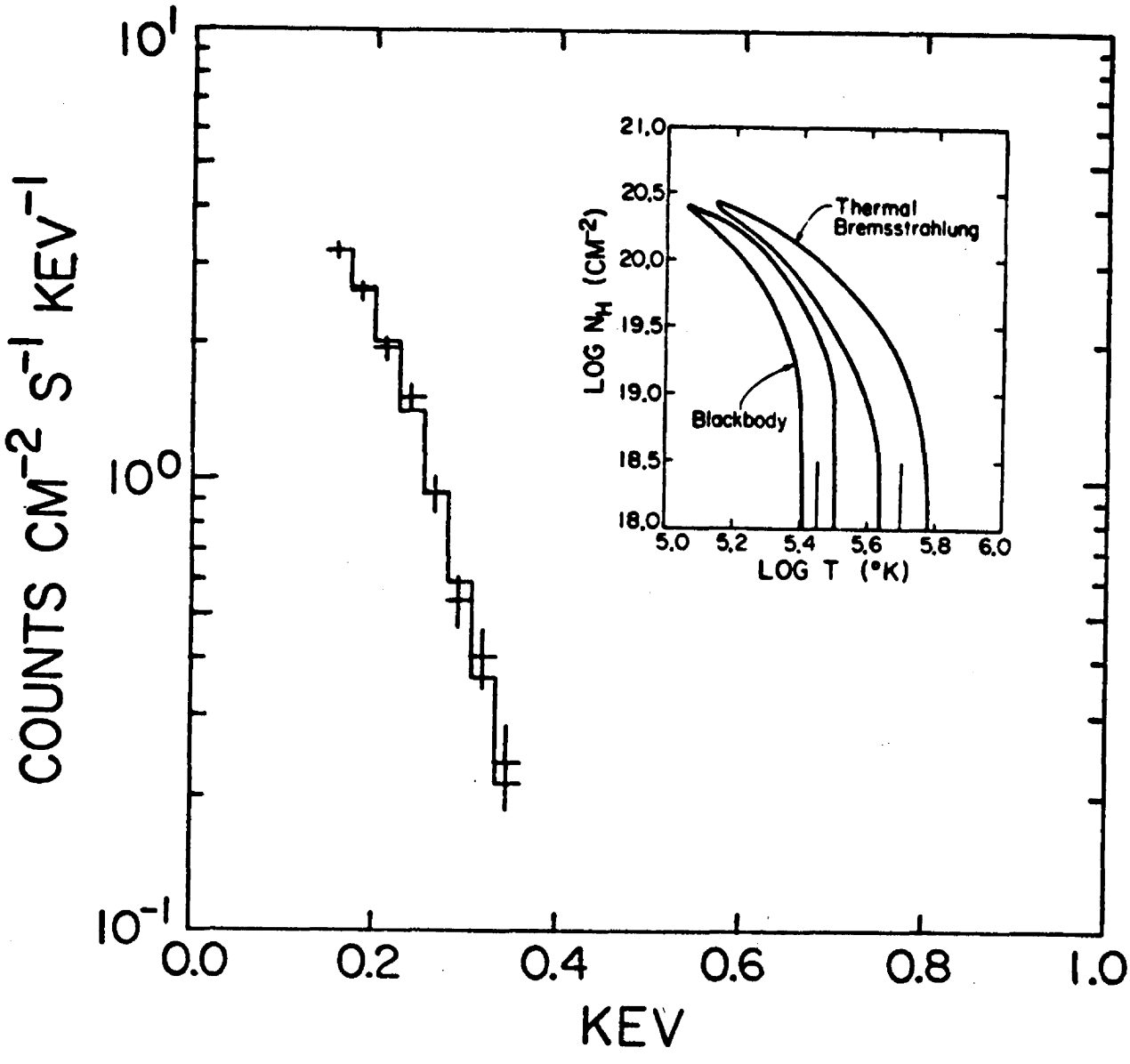

Figure 18. The pulse height spectrum of U Gem versus energy. The object is relatively cool.

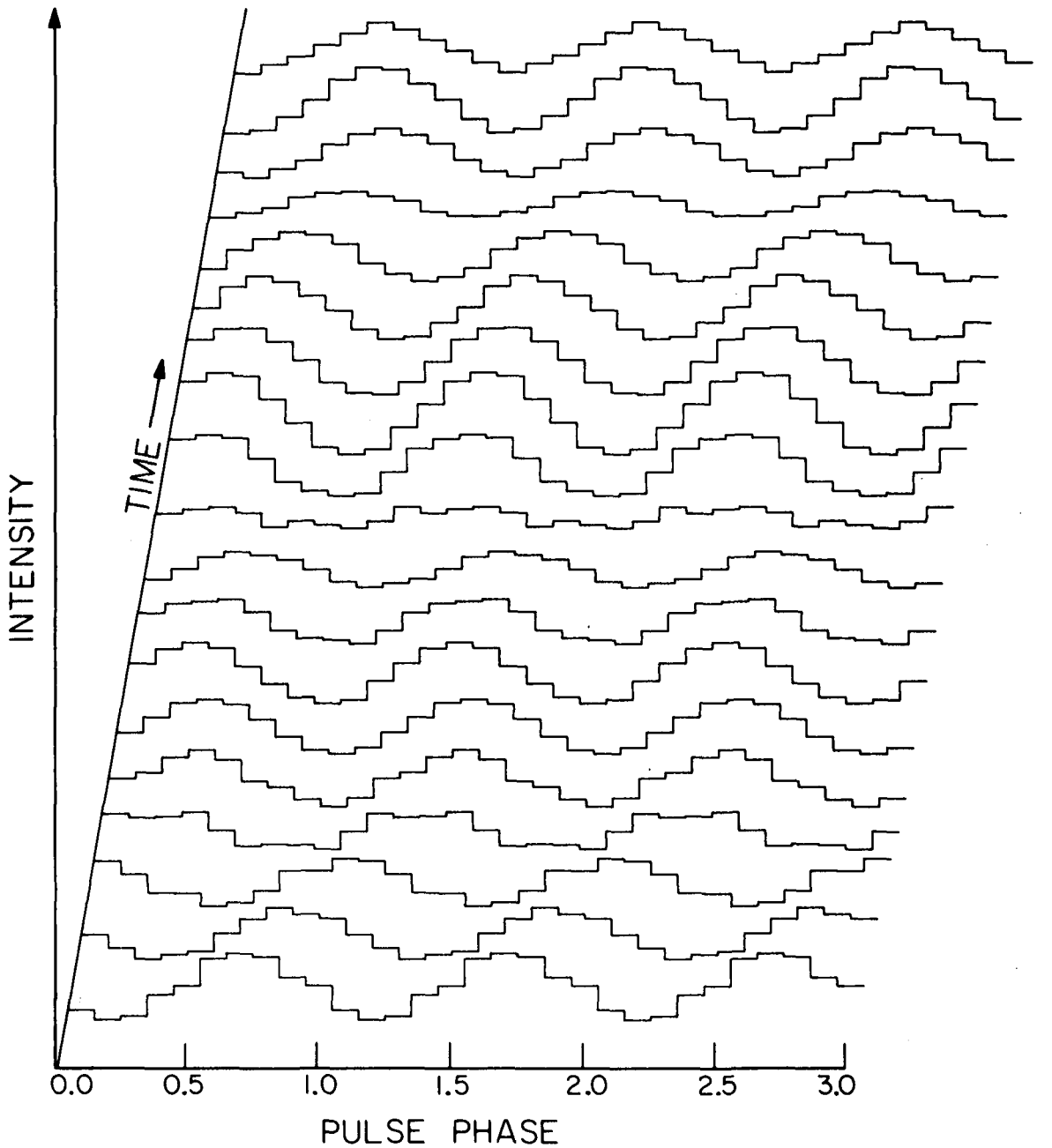

Figure 19. A plot of the SS Cygni pulsations repeated three times per line. Each line is about 15 pulses superposed at a constant period. The lines are consecutive in time.

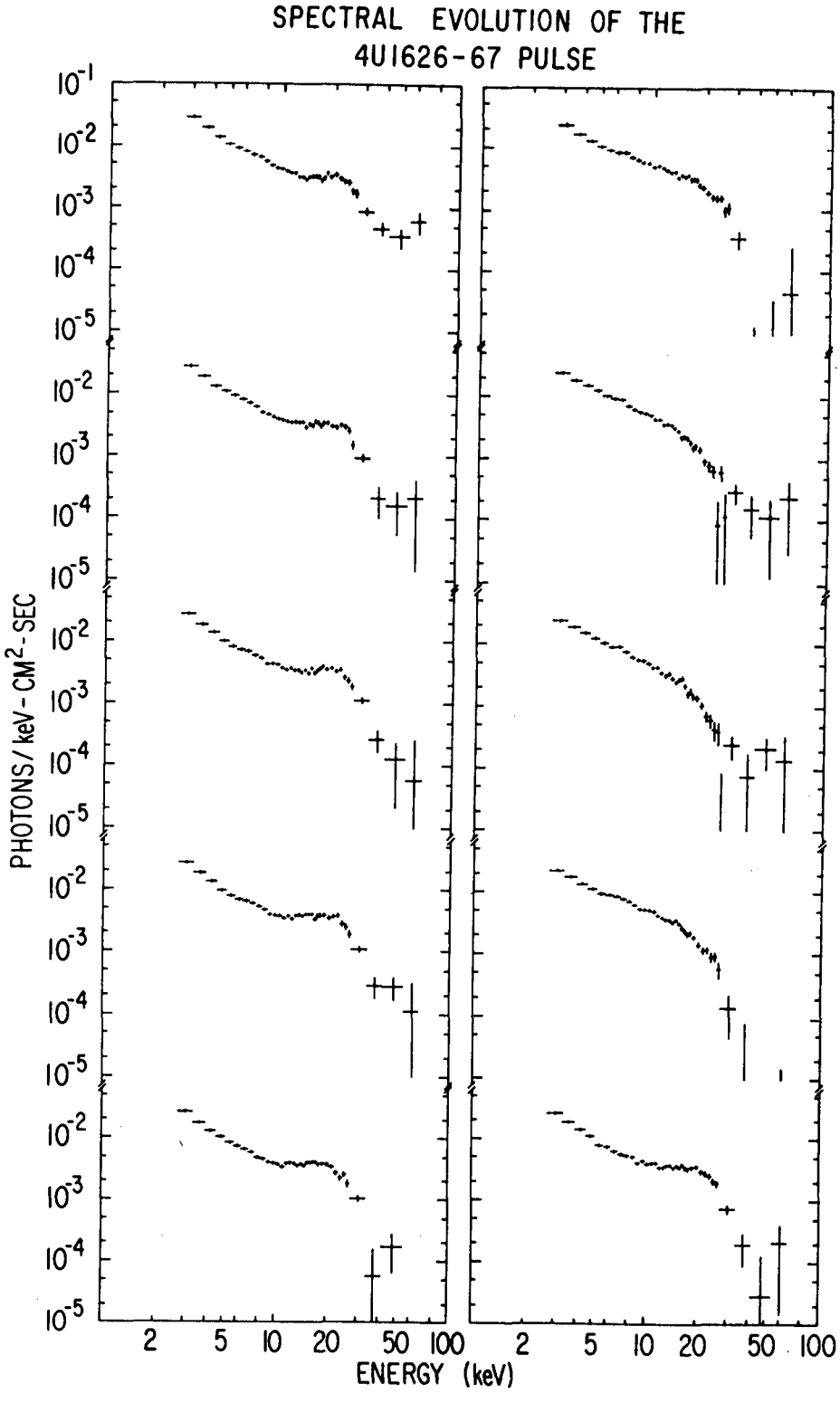

Figure 20. The pulse phase spectra of 4U 1626-67. Ten phase bins are shown representing 0.7 sec of the 7 sec period of the source. Note the feature at ~ 19 keV and the change of shape of the spectrum versus phase. Read down the first column and then down the second for the sequence.

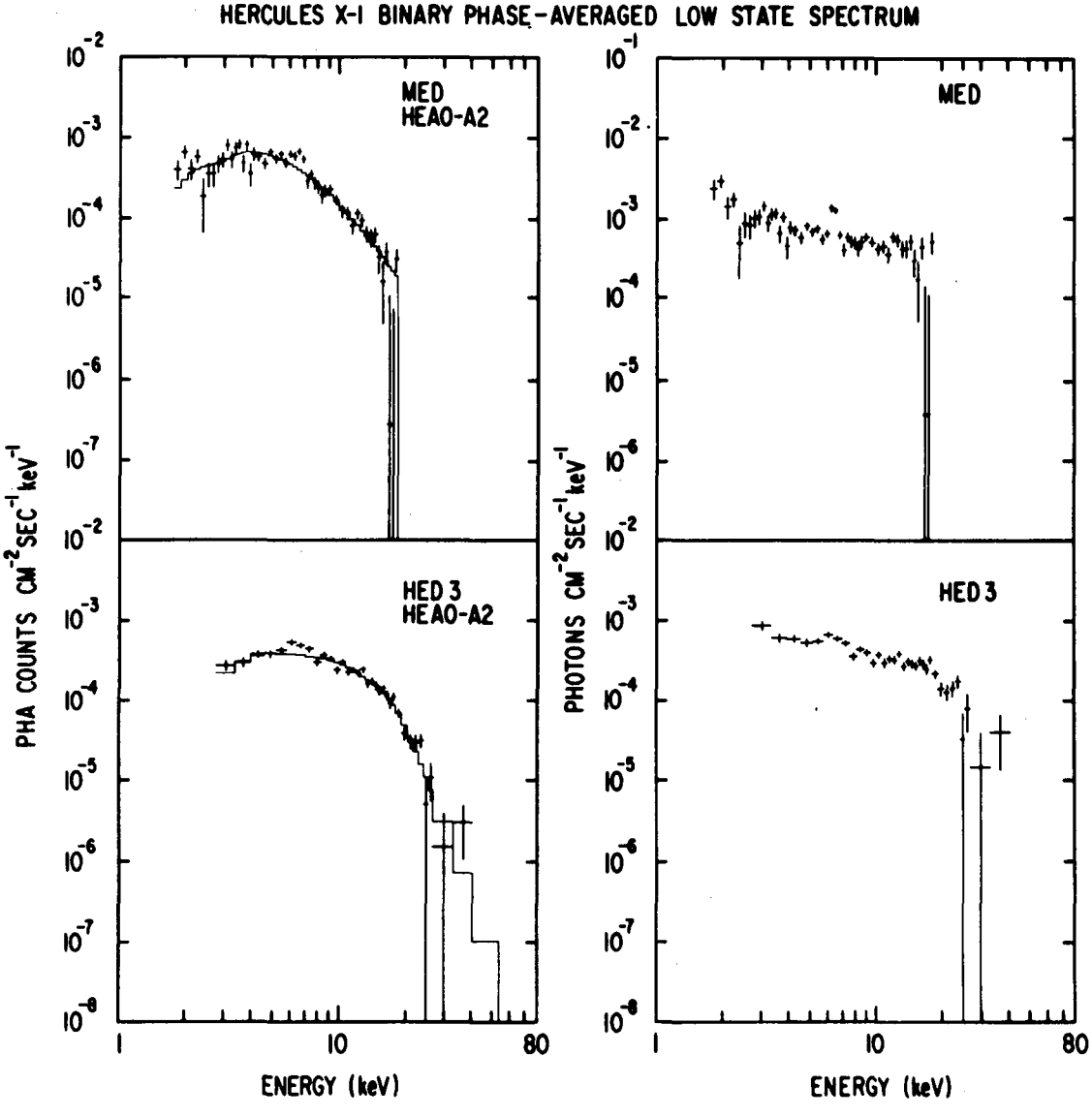

Figure 21. The low-state spectrum of Her X-1 from Pravdo et al. (1978).

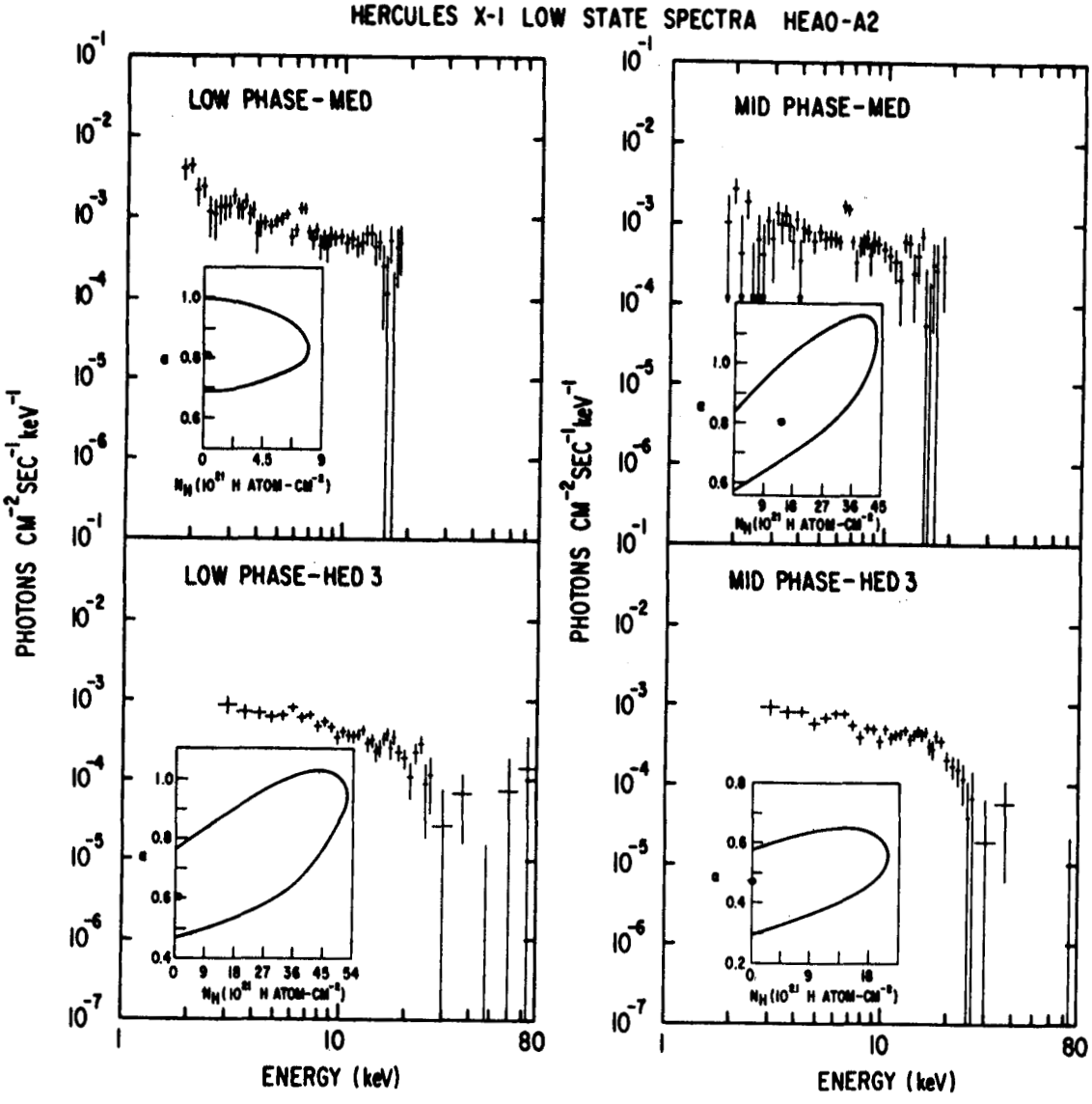

Figure 22. Fits to the low-state spectrum of Her X-1 at the beginning of the orbital binary phase (near phase zero) and toward the middle of the 1.7 day period.

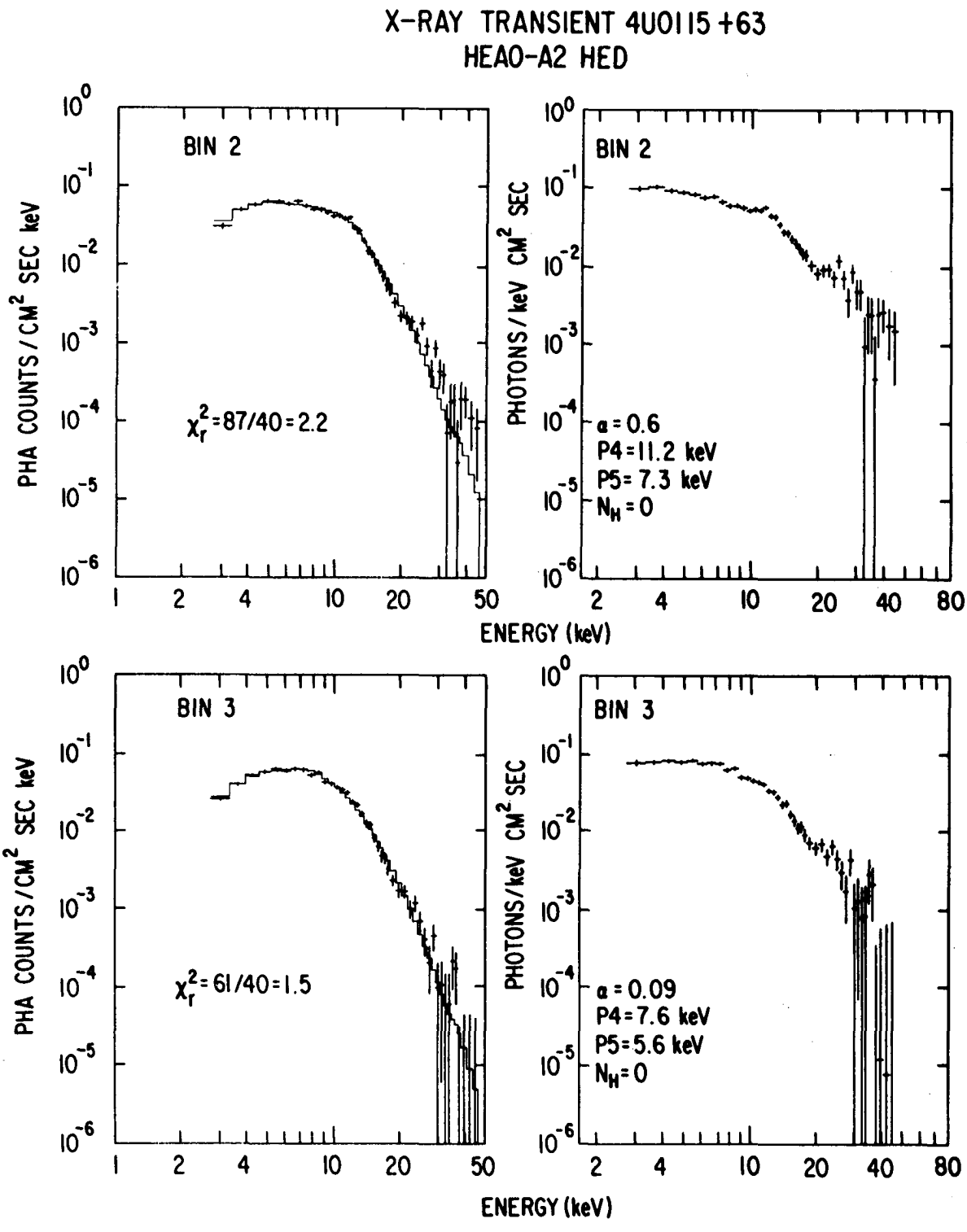

Figure 23. The spectrum of 40-0115+63, an X-ray transient with a 3.6 sec period and a hard X-ray spectrum in two of ten phase bins during the rotation of the neutron star.

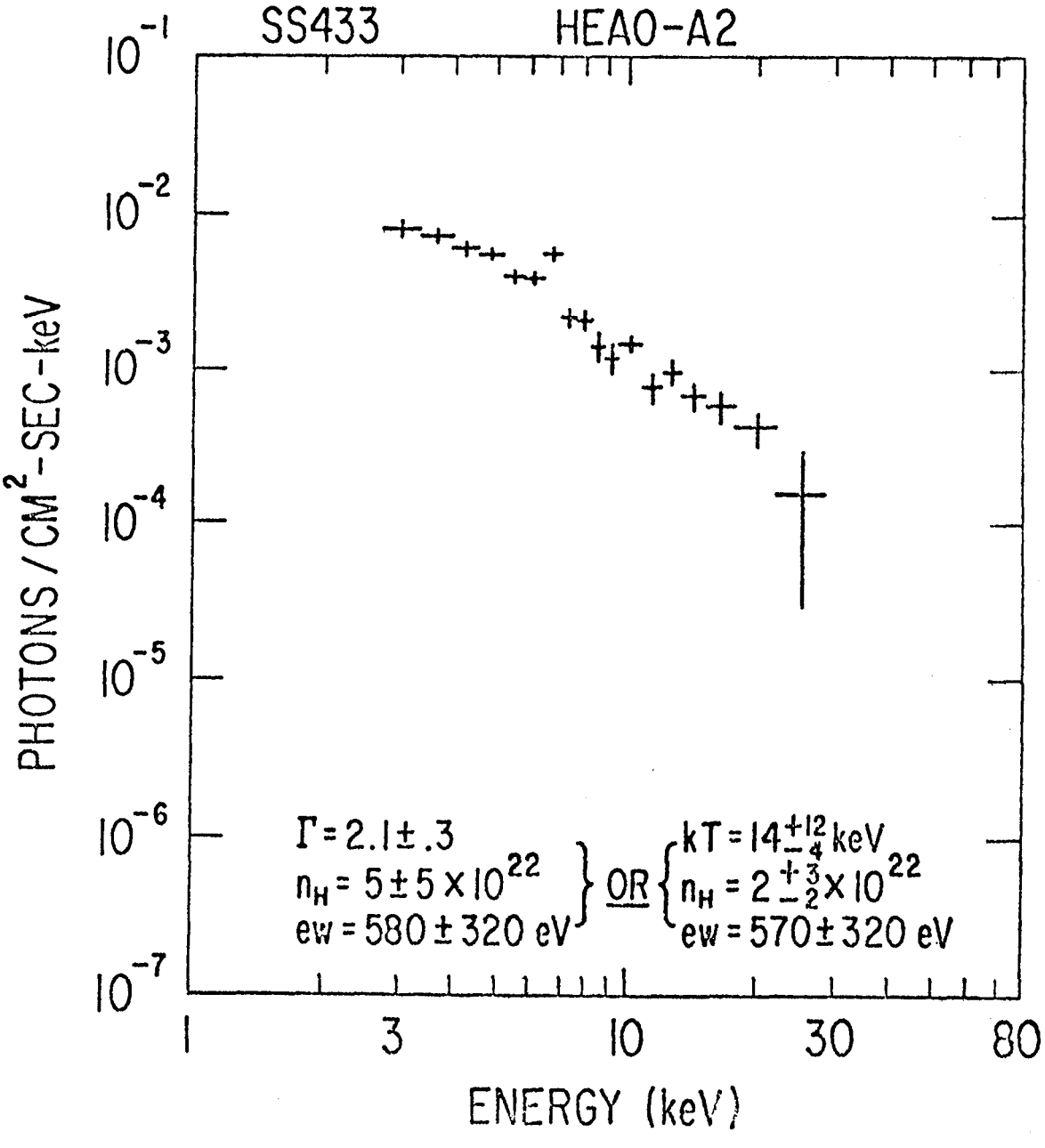

Figure 24. The deduced photon spectrum of SS433. Note the iron-line feature at 6.5 keV.